PB81-205932

Monitoring Techniques for Carbon Fiber Emissions: Evaluation A

GCA Corp.
Bedford, MA

Prepared for

Environmental Sciences Research Lab.
Research Triangle Park, NC

Mar 81

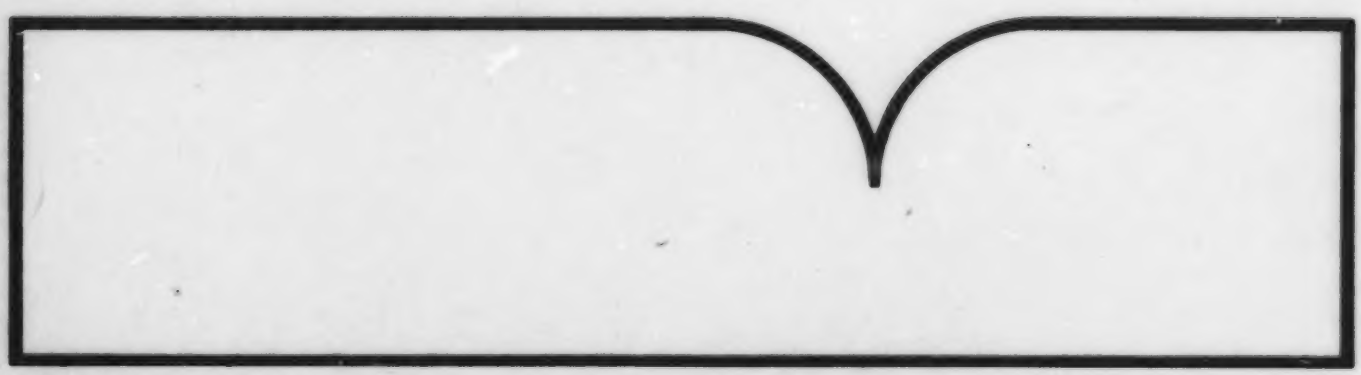

U.S. Department of Commerce
National Technical Information Service
NTIS

BEGIN FIRST LINE OF TEXT HERE
TYPING GUIDE SHEET
CENTER OF PAGE
TOP OF IMAGE AREA
DROPPED HEAD; BEGIN SECTIONS HERE

EPA 600/2-81-048
March 1981

PB81-205932

MONITORING TECHNIQUES FOR CARBON FIBER EMISSIONS
Evaluation A

by

Pedro Lilienfeld
GCA CORPORATION
GCA/TECHNOLOGY DIVISION
Bedford, Mass. 01730

6-1/2"
9-1/8"

Contract No. 68-02-3274

Project Officer

William D. Conner
Emission Measurement and Characterization Division
Environmental Sciences Research Laboratory
Research Triangle Park, North Carolina 27711

ENVIRONMENTAL SCIENCES RESEARCH LABORATORY
OFFICE OF RESEARCH AND DEVELOPMENT
U.S. ENVIRONMENTAL PROTECTION AGENCY
RESEARCH TRIANGLE PARK, NORTH CAROLINA 27711

BEGIN LAST LINE OF TEXT
BOTTOM OF IMAGE AREA, OUTSIDE DIMENSION FOR TABLES AND ILLUSTRATIONS
PRODUCT OF:
NATIONAL TECHNICAL INFORMATION SERVICE
U.S. DEPARTMENT OF COMMERCE
SPRINGFIELD, VA. 22161
3/8"
PAGE NUMBER
EPA-287 (Cin.)
(4-76)

TECHNICAL REPORT DATA
(Please read Instructions on the reverse before completing)

1. REPORT NO.	2.	3. RECIPIENT'S ACCESSION NO.
EPA-600/281-048		PB81 205932

4. TITLE AND SUBTITLE	5. REPORT DATE
MONITORING TECHNIQUES FOR CARBON FIBER EMISSIONS Evaluation A	March 1981 6. PERFORMING ORGANIZATION CODE
7. AUTHOR(S)	8. PERFORMING ORGANIZATION REPORT NO.
Pedro Lilienfeld	
9. PERFORMING ORGANIZATION NAME AND ADDRESS	10. PROGRAM ELEMENT NO.
GCA Corporation GCA/Technology Division Bedford, Massachusetts 01730	C07A1D/03-0630 FY-80 11. CONTRACT/GRANT NO. Contract 68-02-3274
12. SPONSORING AGENCY NAME AND ADDRESS	13. TYPE OF REPORT AND PERIOD COVERED
Environmental Sciences Research Laboratory - RTP, NC Office of Research and Development U.S. Environmental Protection Agency Research Triangle Park, N. C. 27711	14. SPONSORING AGENCY CODE EPA/600/09

15. SUPPLEMENTARY NOTES

16. ABSTRACT

An investigation was carried out of methods and techniques applicable to the detection and monitoring of carbon fibers as they are emitted in processes involving their manufacture or their use. The specific activities of these programs were: (a) to perform a detailed literature search on relevant information about candidate measurement methods, (b) to determine the typical effluent conditions under which carbon fibers are emitted to the atmosphere, (c) to evaluate the various applicable candidate monitoring techniques, (d) to perform a comparison of these methods, and (e) to select a preferred monitoring technique. The following conclusions were reached: (a) routine carbon fiber emissions to the atmosphere are, at present, negligible; (b) no extant instrument is capable of selective detection and measurement of carbon fiber aerosols; and (c) techniques can be developed to provide a practical instrumental solution to carbon fiber monitoring.

Among the most promising candidate techniques identified within this investigation is the photothermal detection method. This approach is discussed in detail, and preliminary design criteria for an instrument incorporating this technique have been developed.

17. KEY WORDS AND DOCUMENT ANALYSIS

a. DESCRIPTORS	b. IDENTIFIERS/OPEN ENDED TERMS	c. COSATI Field/Group

18. DISTRIBUTION STATEMENT	19. SECURITY CLASS *(This Report)*	21. NO. OF PAGES
RELEASE TO PUBLIC	UNCLASSIFIED	85
	20. SECURITY CLASS *(This page)*	22. PRICE
	UNCLASSIFIED	

EPA Form 2220-1 (Rev. 4-77) PREVIOUS EDITION IS OBSOLETE

BEGIN FIRST LINE OF TEXT HERE
TYPING GUIDE SHEET
CENTER OF PAGE
TOP OF IMAGE AREA
DROPPED HEAD; BEGIN SECTIONS HERE
6-1/2"
6-1/8"
BEGIN LAST LINE OF TEXT
3/8"
BOTTOM OF IMAGE AREA; OUTSIDE DIMENSION FOR TABLES AND ILLUSTRATIONS
PAGE NUMBER
EPA-287 (Cin.)
(4-76)

DISCLAIMER

This report has been reviewed by the Environmental Sciences Research Laboratory, U.S. Environmental Protection Agency, and approved for publication. Approval does not signify that the contents necessarily reflect the views and policies of the U.S. Environmental Protection Agency, nor does mention of trade names or commercial products constitute endorsement or recommendation for use.

BEGIN FIRST LINE OF TEXT HERE
TYPING GUIDE SHEET
CENTER OF PAGE
TOP OF IMAGE AREA
DROPPED HEAD: BEGIN SECTIONS HERE

ABSTRACT

An investigation was carried out of methods and techniques applicable to the detection and monitoring of carbon fibers as they are emitted in processes involving their manufacture or their use. The specific activities of these programs were: (a) to perform a detailed literature search on relevant information about candidate measurement methods, (b) to determine the typical effluent conditions under which carbon fibers are emitted to the atmosphere, (c) to evaluate the various applicable candidate monitoring techniques, (d) to perform a comparison of these methods, and (e) to select a preferred monitoring technique. The following conclusions were reached: (a) routine carbon fiber emissions to the atmosphere are, at present, negligible; (b) no extant instrument is capable of selective detection and measurement of carbon fiber aerosols; and (c) techniques can be developed to provide a practical instrumental solution to carbon fiber monitoring.

Among the most promising candidate techniques identified within this investigation is the photothermal detection method. This approach is discussed in detail, and preliminary design criteria for an instrument incorporating this technique have been developed.

This report was submitted in fulfillment of Contract No. 68-02-3274 by GCA Corporation, Technology Division, under the sponsorship of the U.S. Environmental Protection Agency. This report covers the period October 1979 to October 1980.

BEGIN LAST LINE OF TEXT
BOTTOM OF IMAGE AREA OUTSIDE DIMENSION FOR TABLES AND ILLUSTRATIONS
3/8"

EPA-287 (Cin.)
(4-76)

BEGIN FIRST LINE OF TEXT HERE
TYPING GUIDE SHEET
CENTER OF PAGE
TOP OF IMAGE AREA
DROPPED HEAD; BEGIN SECTIONS HERE

CONTENTS

Abstract iii

Figures vii

Tables viii

1. Introduction 1
2. Conclusions 3
3. Carbon Fibers - Properties and Release Mechanisms 5
   General considerations 5
   Fiber structure 10
   Optical absorption 10
   Emissions from carbon fiber production 10
4. Carbon Fiber Sampling Aerodynamics 13
5. Methods of Carbon Fiber Detection and Monitoring 22
   High voltage spark system 22
   Brass ball technique 27
   Low voltage grid system 28
   Continuous optical counter 29
   Lidar 29
   Microwave 29
   Sticky tape 29
   Filter technique 30
   Spectrophone 30
   The micro-raman technique 31
   Optical attenuation 32
   Light scattering methods 32
   Light polarization 34
   Differential conductivity sensing 34
   Differential electric mobility 34
   Electric alignment of fibrous-shaped particles 34
   Magnetic alignment of fibrous-shaped particles 35
   Aerodynamic alignment of fibers 35
   Ultrasonic effects 35
   Microscopy and video analysis of collected samplers . . . 35
   Spark discharge spectrometry 36
   Laser flashing - spark spectrometry 36
   Scintillating particle analysis 37
   X-ray techniques 37
   Differential light scattering 37
   Fiber detection by LISMEFA 38
   Airborne carbon fiber in-situ monitoring by photo-thermal detection 47

BEGIN LAST LINE OF TEXT
BOTTOM OF IMAGE AREA OUTSIDE DIMENSION FOR TABLES AND ILLUSTRATIONS
3/8"

Preceding page blank

PAGE NUMBER
EPA-287 (Cin.)
(4-76)

BEGIN FIRST LINE OF TEXT HERE
TYPING GUIDE SHEET
CENTER OF PAGE
TOP OF IMAGE AREA
DROPPED HEAD; BEGIN SECTIONS HERE
BEGIN LAST LINE OF TEXT
BOTTOM OF IMAGE AREA OUTSIDE DIMENSION FOR TABLES AND ILLUSTRATIONS
3/8"
PAGE NUMBER
EPA-287 (Cin.)
(4-76)

CONTENTS (continued)

6. Applicability and Cost Analysis of Candidate Methods 58

References 62
Bibliography 75

FIGURES

Number		Page
1	Gravitational settling velocity of graphite fibers as function of fiber diameter and length	15
2	Effect of velocity ratio on concentration ratio for a sampling tube oriented in the direction of the mainstream flow	17
3	Expanded 90° probe bend designed to minimize inertial particle losses	18
4	Nomograph for estimating gravitational settling losses in horizontal cylindrical ducts	20
5	Spark discharge circuit schematic diagram	23
6	Typical discharge current waveform as recorded by an oscilloscope	25
7	Schematic of the optical attenuation apparatus	33
8	LISMEFA detection configuration	39
9	Degree of conductive fiber orientation for an oscillation electric field at 400 Hz, whose configuration follows that of Figure 8	41
10	Typical FAM-1 carbon fiber pulse trains	43
11	FAM-1 optics-flow diagram	44
12	FAM-1 overall block diagram	46
13	Black-body emission as a function of wavelength and absolute temperature	52
14	Simplified conceptual sensing system diagram of light scattering-photothermal carbon fiber monitor	55
15	Conceptual signal flow chart of a photo-thermal-light-scattering carbon fiber monitoring system	57

TABLES

Number		Page
1	Typical Properties of Carbon Fibers	8
2	Relevant Physical and Operational Parameters of Spark System .	27
3	Summary Tabulation of Potentially Applicable Techniques to the Detection and Measurement of Carbon Fibers, Including a Qualitative Cost Analysis	59

TYPING GUIDE SHEET
BEGIN FIRST LINE OF TEXT HERE
CENTER OF PAGE
TOP OF IMAGE AREA
DROPPED HEAD: BEGIN SECTIONS HERE

SECTION 1

INTRODUCTION

Recent years have seen the rapidly growing importance of carbon and graphite composites in their application to high-strength materials in aircraft, automobiles, military hardware and other uses. The promise of drastic reductions in weight, and other significant advantages, as results of the replacement of steel and aluminum by these composites has stimulated their development and optimization at a rapidly accelerating pace. A significant drawback of this material, however, has been recently identified: inadvertent combustion of such a composite can result in large-scale aerosolization of the carbon or graphite fibers embedded in the composite binder. The release and airborne transport of these fibers, whose length may reach 20 mm, has been found to cause serious effects on electrical and electronic equipment as a result of the relatively low electrical resistivity of these fibers. Spark-over, shorting, degradation of insulation, circuit impedance alteration, and secondary effects accompanying such primary ones have created an understandable concern about potential catastrophic results of any massive release of this type (e.g., aircraft crash, etc.) affecting a wide urban and/or industrial area.

The identification of this problem has led several governmental agencies to devote an appreciable effort to its complete characterization and eventual solution. The EPA has been charged with the coordination of efforts directed at the development of instrumentation for continuous source monitoring of airborne graphite fibers.

Until fairly recently, monitoring of fibrous-shaped aerosol particles was exclusively performed by means of filter sampling and subsequent microscope counting of the collected particles. This is a tedious, noncontinuous, non-realtime method that has been established as the standard procedure to determine worker exposure to asbestos fibers in industrial and mining environments. This same approach can and has been applied to determine the concentration of carbon and graphite fibers, but although phase-contrast microscopy is not required for these latter fibers, the above-mentioned disadvantages of the filter-microscopy method remain essentially invariant.

The objective of this program was to investigate methods and techniques applicable to the detection and monitoring of carbon fibers as they are emitted in processes involving their manufacture or their use. The specific activities of this program were: (a) to perform a detailed literature search on relevant information about candidate measurement methods, (b) to determine the typical effluent conditions under which carbon fibers are emitted to the

BEGIN LAST LINE OF TEXT
BOTTOM OF IMAGE AREA OUTSIDE DIMENSION FOR TABLES AND ILLUSTRATIONS
3/8"
PAGE NUMBER
EPA-2ET (Cin.)
(4-76)

atmosphere, (c) to evaluate the various candidate monitoring techniques applicable to this problem, (d) to perform comparative cost estimates of these methods, and (e) to select a monitoring technique that shows the greatest promise of providing a useful, practical and cost-effective solution to the measurement of carbon fiber emissions.

This investigation constituted the first phase of an overall program directed at the development of a prototype monitoring system capable of selective source detection and monitoring of airborne carbon fibers.

SECTION 2

CONCLUSIONS

Several important conclusions were reached within this program. These conclusions relate to the various areas investigated as part of this project: (a) the review of candidate monitoring methods, (b) the determination of the conditions and magnitude of carbon fiber emissions, and (c) the relative merits of the potentially applicable monitoring techniques.

The reluctance of some carbon-fiber and related products manufacturers to provide answers and relevant information constituted a distinct hindrance in some cases. Letters had to be written to those organizations that refused to provide verbal telephone information, and even then the responses were often of limited value, or absent altogether.

One of the central corollaries derived from the information research performed within this program is that routine emissions of carbon fibers from manufacturing operations are, in general, of negligible importance; i.e., the emission rate of carbon fibers into the atmosphere resulting from the normal production activities does not warrant, at the present time, an intensive monitoring program. Incidental and uncontrolled carbon fiber releases, however, remain a matter of concern.

Future drastic intensification of the industrial volume of production of carbon fibers and related products may, however, modify this situation sufficiently to warrant a careful reassessment of the above presented conclusions. It appears, at this time, that instrumentation for in-plant monitoring as well as ambient monitoring of carbon fibers may be required in order to reduce or prevent electrical equipment failure within industrial environments, as well as to provide adequate means to assess the potential damaging effects of open and uncontrolled combustion of carbon-fiber containing materials.

The second major conclusion, reached as a result of the study under consideration, is that no airborne carbon fiber detection and monitoring instrument is presently available capable of unambiguous identification and measurement of such fibers, in the concomitant presence of other aerosols.

The third important inference derived from this study is that there are sensing and detection techniques which, if properly developed for the specific objective under consideration, can provide unequivocal and selective methodology for the continuous automated monitoring of airborne carbon fibers, in the presence of other contaminating particles. It appears feasible that such

BEGIN FIRST LINE OF TEXT HERE
TYPING GUIDE SHEET
CENTER OF PAGE
TOP OF IMAGE AREA
DROPPED HEAD. BEGIN SECTIONS HERE
6-1/2"
6"/6"
BEGIN LAST LINE OF TEXT
BOTTOM OF IMAGE AREA OUTSIDE DIMENSION FOR TABLES AND ILLUSTRATIONS
3/6"
PAGE NUMBER
EPA-287 (Cin.)
(4-76)

a technique, or combination of techniques, may be applicable to in-plant, emission testing, and ambient monitoring applications. The most promising of these techniques is: a photo-thermal-electric alignment method, combined with light scattering characterization.

BEGIN FIRST LINE OF TEXT HERE
TYPING GUIDE SHEET
CENTER OF PAGE
TOP OF IMAGE AREA
DROPPED HEAD: BEGIN SECTIONS HERE

SECTION 3

CARBON FIBERS - PROPERTIES AND RELEASE MECHANISMS

GENERAL CONSIDERATIONS

In the period 1963-1965, it was discovered that very high strength filaments could be obtained by subjecting a precursor fiber to a rigidly controlled tensile stress during high temperature pyrolization. Technically, the term "carbon fiber" applies to fibers which have been pyrolized at temperatures of 1100°C to 1200°C, and the term "graphite fiber" applies to those carbon fibers which have been heat treated at temperatures on the order of 2200°C to 2700°C. In practice, however, the two terms are often used interchangeably to describe the high-stiffness carbon-based fibers.

Individual fibers are about 8 μm in diameter and are produced in the form of yarns, each strand containing thousands of individual fibers. The chemical and physical properties that produce strength and stiffness characteristics also result in very high electrical conductivity for the fiber. The very high temperatures at which fibers are formed ensure their virtual indestructibility under most conditions.

The singular properties of carbon/graphite fibers become of practical interest when they are translated into a useful form through consolidation with a matrix (binder), into a composite material. Studies based on experience gained from R&D programs and production of advanced composite aerospace structures indicate that utilization of graphite fiber composites in aircraft can add strength and reduce weight and thus provide significant benefits in cost and performance.

The high electrical conductivity of the carbon/graphite fibers is the prime factor in their negative effects on electrical equipment;[1] however, other properties such as small fiber diameter, generally short length and low density are also important contributing factors. These latter fiber characteristics permit any small movement of air to cause free fibers to become airborne and to be transported over relatively long distances by normal atmospheric motion. Because of their high conductivity, carbon/graphite fibers which settle on or across electrical contracts or circuits can cause effects which could damage equipment or cause it to malfunction. They can cause: (1) resistive loading; (2) temporary shorts; or (3) electrical arcing.

Many industrial plants producing and using free fibers have experienced malfunctions of electrical and electronic equipment and, in some cases, resultant fires. These industries have found it possible to limit such problems by controlling the fibers in production and by instituting protective

BEGIN LAST LINE OF TEXT
BOTTOM OF IMAGE AREA; OUTSIDE DIMENSION FOR TABLES AND ILLUSTRATIONS
3/8"

PAGE NUMBER
EPA-287 (Cin.) (4-76)

BEGIN FIRST LINE OF TEXT HERE
TYPING GUIDE SHEET
CENTER OF PAGE
TOP OF IMAGE AREA
DROPPED HEAD; BEGIN SECTIONS HERE

measures for electrical equipment and circuits. Such measures include eliminating exposed conductors, covering conductors with conformal coating, or providing fan filters. Similar problems have not been experienced by industries which receive and use the carbon/graphite fibers after they have been "pre-impregnated" with a plastic binder or fully consolidated in the form of a composite.

There are situations in which carbon/graphite fibers can be released from composites. Burning of a composite material followed by mechanical agitation can release a fraction of the carbon/graphite as single fibers or as lint.

Waste disposal by incineration of either industrial scrap or discarded composite products represents a possible source of free carbon/graphite fibers capable of causing electrical effects. Accidental fires in vehicles (aircraft or automobiles) incorporating significant amounts of carbon/graphite fiber composites are other major potential sources of free fibers.

Limited test data[1] indicate that electrical equipment tolerance to free carbon/graphite fiber interference can be characterized in terms of exposure, or (fibers/m^3) sec; electrical interference seems to begin in the exposure range of 10^4 -10^7 (fibers/m^3) sec.

Studies have demonstrated the high resistance of graphite fiber products to combustion at temperatures up to 1000°C.[1] There is no doubt that the disposal of graphite fiber composite waste materials by conventional refuse incineration would result in the release of airborne graphite fiber residues. Released fibers will be intact in some instances and partly degraded and thinned in others. The resistance of carbon fibers to incineration is dependent on their degree of graphitization. It is clear that the control of carbon fiber emissions from the incineration of waste composite materials will require either high efficiency fiber trapping or incinerator designs that permit more complete combustion of fibers.

Although free graphite fibers may be released by the sawing or drilling of composite materials, these generally have lengths less than 100 μm and are therefore likely to have a very low potential for causing electrical equipment failure.[1] On the other hand, fibers released by these and other types of machining operations (cutting, grinding, etc.) are in a size range that requires an assessment of potential health hazards. Since most of the fibers generated have diameters (about 6-8 μm) that are predetermined in the fiber manufacturing process, their health effects are likely to be limited to skin, eye, and upper respiratory tract irritation. However, the evidence that longitudinal cleavage of fibers can occur[1] requires that due considerations be given to the possible generation, during manufacturing operations, of significant numbers of smaller diameter fibers which can penetrate more deeply into the lungs and therefore constitute a greater respiratory hazard.

Carbon fiber samples include fibers with a broad range of physical properties in terms of tensile strength and elasticity, thus reflecting varying degrees of graphitization. Properties of composites are dependent not

BEGIN LAST LINE OF TEXT
BOTTOM OF IMAGE AREA; OUTSIDE DIMENSION FOR TABLES AND ILLUSTRATIONS
3/8"

EPA-287 (Cin.)
(4-76)

BEGIN FIRST LINE OF TEXT HERE
TYPING GUIDE SHEET
CENTER OF PAGE
TOP OF IMAGE AREA
DROPPED HEAD; BEGIN SECTIONS HERE

only on fiber characteristics but also on fiber surface treatment, type of resin matrix, proportions and geometry of the fiber-matrix combination and resin curing procedure.

Scanning electron micrographs show that the fibers appear to be smooth circular cylinders with diameters varying from about 5 to 8 μm, though the actual cross-sectional morphology of different samples vary and include circular, elliptical and dogbone shapes. Some manufacturers expose fiber surfaces to a roughing etch to improve interlaminar sheer strength in the composite. Also, a sizing or coating of resin is often added to enhance the bonding capability of the fibers in the composite medium.

Incineration Effects

Exposure of raw carbon fiber samples to temperatures of 200° to 220°C for 30 to 60 minutes causes little or no damage. There are no discernible changes in the appearance of the fibers when observed in the SEM. At a temperature of 1000°C, however, the fibers show definite signs of degradation after a short period. Dimples or pits in the fibers appear after 1 minute and are deep and numerous after 3 1/2 minutes. A general thinning of the fibers even in undimpled portions has also been noted.

When samples of carbon fiber composite in epoxy resin matrices are subjected to elevated temperatures, the epoxy matrix material is incinerated first, leaving the fibers virtually intact at temperatures of 300 - 600°C and delaying the degradation of fibers at 1000°C.[2] Examination of composite samples after 5 minutes at 1000°C showed some charred remains of the epoxy matrix adhering to apparently unaffected fibers as well as some fiber clusters completely free of epoxy residue with little, if any, significant damage to the fibers.

Another type of carbon fiber product subjected to incineration has been a woven cloth (Panex PWB-6 manufactured by Stackpole) designed for high heat resistance. After exposure for 23 minutes at 1000°C, the cloth fibers were still in remarkably good condition though showing very definite signs of damage including thinning and pitting.[2]

Machining Effects

Microscopic examination of dust generated by drilling a sample of composite (Fortafil 3U manufactured by Great Lakes Carbon) show the presence of free fibers in lengths mainly from about 50 to 100 μm in addition to particles of epoxy debris.[2]

Dust from sawing another sample of composite (Magnamite A 370-84/3501-6 manufactured by Hercules) also contained free fiber fragments.[2] These are generally shorter than those seen in drill dusts, and the micrographs also show evidence that some were cleaved longitudinally, probably along the graphitic planes.

BEGIN LAST LINE OF TEXT
BOTTOM OF IMAGE AREA, OUTSIDE DIMENSION FOR TABLES AND ILLUSTRATIONS
3/8"

EPA-287 (Cin.)
(4-76)

BEGIN FIRST LINE OF TEXT HERE
TYPING GUIDE SHEET
CENTER OF PAGE
TOP OF IMAGE AREA
DROPPED HEAD: BEGIN SECTIONS HERE

Carbon Fiber Properties

General Aspects--

The physical properties of carbon and graphite fibers are important in the determination of their electrical, mechanical and thermal behavior as related to the sensing methodology discussed in this report. There are, of course, no "standard" types of such fibers; i.e., a range of variability exists depending on the manufacturing process and the characteristics of the original material from which these fibers are made.

Table 1 is a summary of the most important properties and their typical values, or range of values, obtained from various relevant sources.

TABLE 1. TYPICAL PROPERTIES OF CARBON FIBERS

Diamagnetic susceptibility	5×10^{-6}
Index of refraction:	
Real part	1.8 to 2.7
Imaginary part	0.7 to 1.6
Tensile strength	1.4×10^{9} pascal
Tensile modulus	2.4×10^{11} pascal
Density amorphous carbon	1.8×10^{3} to 2.1×10^{3} kg m^{-3}
Density graphite	1.9×10^{3} to 2.3×10^{3} kg m^{-3}
Electrical resistivity	1.2×10^{-5} to 1.4×10^{-5} Ωm
Diameter	5 to 10 μm
Typical length range	100 μm to 20 mm
Specific heat	711 joule kg^{-1} $^{o}K^{-1}$
Melting point	$3823^{o}K$ (graphite sublimes at $3640^{o}K$)
Boiling point	$5100^{o}K$
Ignition temperature in air	$673^{o}K$
Carbon assay	92 to 99 percent
pH	6

Carbon fibers of Young Modulus 410 GN m^{-2} (60×10^{6} lb in^{-2}) consist of graphite crystallites (L_a about 9 nm) with their basal planes having a preferred orientation of within 10^{o} to the fiber axis. They are made by the pyrolysis of polyacrylonitrile textile fibers. Intermolecular reactions occur between the polymer chains and, by maintaining the chains parallel to the fiber axis by tension in the early stages of pyrolysis, a primitive oriented structure arises which becomes an oriented graphite structure at higher temperatures. Stereochemical factors are important and since the textile fiber contains fibrils of about 15 nm width, with distinct boundaries, the

BEGIN LAST LINE OF TEXT
BOTTOM OF IMAGE AREA, OUTSIDE DIMENSION FOR TABLES AND ILLUSTRATIONS
3/8"

EPA-287 (Cin.) (4-76)

BEGIN FIRST LINE OF TEXT HERE
TYPING GUIDE SHEET
CENTER OF PAGE
TOP OF IMAGE AREA
DROPPED HEAD; BEGIN SECTIONS HERE

pyrolysis reactions are confined within the fibrils so that the carbon fiber also has a fibrillar structure with the oriented graphite crystallites contained within the fibrils.

The mean strength of the carbon fibers, 2.0 GN m^{-2} (300 x 10^3 lbf in^{-2}), is limited by defects; e.g., the mean strength increases as the gauge length decreases. Some of these defects are due to inclusions or voids in the parent fiber. By stretching the carbon fibers at 2700°C, crystallite orientation is increased and the Young modulus rises to about 689 GN m^{-2} (100 x 10^6 lbf in^{-2}).

Carbon fibers are becoming useful in technology because they are light and of high Young modulus and tensile strength in the direction of the fiber axis. It is the unique combination of these properties in one single material that makes them interesting and useful.

The low density is an intrinsic property of the graphite crystal (2.26 g cm^{-3}) as is high modulus, which is high only in the layer planes. The very anisotropic layer lattice of the graphite crystal has an elastic constant parallel to layer planes of

1015 GN m^{-2} (145 x 10^6 lbf in^{-2}),

while the Young modulus in the C axis is only

35 GN m^{-2} (5 x 10^6 lbf in^{-2}).

Hence any polycrystalline carbon fiber must have a high degree of preferred orientation of the layer planes parallel to the fiber-axis.

Fiber Strength--

The Young modulus is an intrinsic property dependent on direction but not on size. Strength is sensitive to defects so therefore the gauge length of the fiber will affect the observed strength.

The average strength increases with decrease in gauge indicative of a random distribution of strength lowering defects and extrapolation to 1 mm length indicates a strength of 3.5 GN m^{-2}. It has been shown that some of these defects are voids or inclusions in the parent fiber carried over into the carbon fiber. The identification and counting of various flaws visible in the parent fiber under the optical microscope has been done, and it is concluded that improvement in fiber cleanliness will increase the carbon fiber strength.

If we look at the standard deviation of the strength of the parent fiber at room temperature, it is 10 percent of the mean with an elongation of about 26 percent, but the same fiber tested at liquid nitrogen temperature has a standard deviation of 26 percent with a very wide range of elongations. This could mean that there are structural defects in the parent fiber which become effective in reducing strength when plastic flow is made more difficult.

BEGIN LAST LINE OF TEXT
BOTTOM OF IMAGE AREA; OUTSIDE DIMENSION FOR TABLES AND ILLUSTRATIONS
3/8"

EPA-287 (Cin.)
(4-76)

BEGIN FIRST LINE OF TEXT HERE
TYPING GUIDE SHEET
CENTER OF PAGE
TOP OF IMAGE AREA
DROPPED HEAD: BEGIN SECTIONS HERE
6-1/2"
BEGIN LAST LINE OF TEXT
3/8"
BOTTOM OF IMAGE AREA; OUTSIDE DIMENSION FOR TABLES AND ILLUSTRATIONS
PAGE NUMBER
EPA-287 (Cin.) [4-76]

FIBER STRUCTURE

X-ray diffraction shows, as expected, that the Young modulus is a function of basal plane orientation and that the crystallites are small, of plane width about 8 nm and of stacking height about 6 nm. The crystallites seem to be present in strings in an internal fibrillar structure derived from the parent fiber. All textile fibers have these long but slender fibrils, width 10 to 20 nm, and low angle diffuse scattering of X-rays reveals long narrow pores between them. These fibril boundaries will be barriers to the intermolecular reactions necessary for development of modules so that they are confined within the fibrils and a carbon pseudomorph of the parent fiber results. Ultra-thin sections cut with a diamond knife give details of internal structure in the electron microscope.

Graphite structure has been generally accepted as hexagonal with a well marked basal cleavage in very thin flakes. Graphite is transparent, uniaxial and negatively birefringent with a refractive index of about 2.0.

OPTICAL ABSORPTION

One of the unique properties of carbon particles and thus of fibers of this material, is the high optical absorption they exhibit in the visible part of the electromagnetic spectrum. Most noncarbonaceous airborne particles encountered in typical emission and ambient situations are of dielectric nature and are thus essentially pure light scatterers. Carbon particles have a complex index of refraction; i.e., with a substantial imaginary component whose magnitude is related to the absorptive properties. Typical values of this complex index of refraction for carbon fibers range from 1.8 to 2.7, for the real part, and 0.6 to 1.6 for the imaginary one, for visible light. This light-absorptive property of carbon has been applied for its detection in collected samples of aerosol particles by means of photoacoustic analysis and will be further discussed in the context of applicable detection methodology.

EMISSIONS FROM CARBON FIBER PRODUCTION

Basic Process

Carbon and graphite fibers are manufactured from precursor fibers, most commonly polyacrylionitrile (PAN), but pitch, tar and rayon fibers are also used as precursors. Pitch and tar can be transformed into a suitable fiber by pyrolysis in a nitrogen atmosphere with subsequent extrusion. Bundles or tows of precursor fibers are wound around frames to maintain a tensile stress during the initial heat treatment step. PAN fibers are heated to 220^{o}C in an oxidizing atmosphere with various degrees of stretching to improve Young's modulus.

The next step in the process is to carbonize the oxidized fibers in an inert atmosphere at temperatures of up to 1500^{o}C. Rayon fibers are also stretched during this stage (or held in tension to prevent shrinkage) to improve tensile strength and stiffness. A final heat treatment step at temperatures of up to 3000^{o}C may be included.

BEGIN FIRST LINE OF TEXT HERE
TYPING GUIDE SHEET
CENTER OF PAGE
TOP OF IMAGE AREA
DROPPED HEAD; BEGIN SECTIONS HERE

Technically, carbon fibers pyrolized at temperatures between 1100° and 1500°C, consist of an amorphous carbon network and exhibit a higher electrical resistivity. Graphite fibers are pyrolyzed at temperatures between 2000° and 3000°C, consist of a crystalline fiber structure, and exhibit a very low electrical resistivity.

Uses

There are two major uses for carbon and graphite fibers: (1) carbon fiber reinforced plastics (CFRP) and (2) carbon fiber reinforced carbon (CFRC). The reinforced plastic may be produced from either resin impregnated carbon-base molding composites or preimpregnated laminates. In either case the plastic parts are produced in molds at temperatures usually less than 165°C and at pressures of about 21-35 kg/cm^2 (300-500 psi). The CFRC is produced by heating carbon fibers in a bulk carbon matrix to 2700°C at ambient pressure in nitrogen, argon and other inert atmospheres. Carbon fibers may be found in the exhaust gases of the CFRC process.

Specific Manufacturers and Their Processes

Stackpole uses a vacuum process to produce carbon and graphite fibers from PAN precursor fibers. Both batch and continuous production processes are used with final heat treatment of fibers at 3000°F (1800°C). Initial off-gases are high in volatiles from precursor fibers--coal tar traps are used to reduce volatiles in exhaust ducts. The process produces peaks of up to 100-150 cfm in exhaust gas flow rates as certain critical temperatures are reached. Exhaust gases are treated by an incinerator operating at ~2000°F; gases enter the incinerator at about 300°-400°F. Nitrogen gas is used at certain points in the process and to cool the fibers in the furnace at the end of the process. Stackpole uses NEMA 12 enclosures on all susceptible electrical equipment.

AVCO produces CFRC from fiber produced by Lowell Division. Carbon fibers in a carbon matrix are heated to 4900°F (2700°C) at ambient pressure in nitrogen gas, argon gas, or are packed in other carbon materials. Exhaust gases from this process are controlled by an afterburner operating at ~2000°F.

Great Lakes Research uses several furnaces to heat the precursor fibers in several stages of increasing temperature. There is a 50 percent precursor fiber weight loss to volatiles in the initial oxidation stage at temperatures up to 1000°C. Any fibers at this stage would be electrically insulating. No significant collections of fibers have been found during cleanout of oxidation offtake ducts. Exhaust gases include volatiles, hydrogen cyanide, nitrogen gas and air from other sources, all of which are ducted to an incinerator and a chemically-active scrubber.

Cooling of fibers occurs in unenclosed areas, and sizing is used to finish the fibers and prevent them from becoming airborne. Packaging of the fibers includes rewinding and/or chopping of the fibers. These areas, which represent the largest potential for airborne fibers, are hooded and ducted to a baghouse.

BEGIN LAST LINE OF TEXT
BOTTOM OF IMAGE AREA; OUTSIDE DIMENSION FOR TABLES AND ILLUSTRATIONS
3/8"

EPA-287 (Cin.)
(4-76)

BEGIN FIRST LINE OF TEXT HERE
TYPING GUIDE SHEET
CENTER OF PAGE
TOP OF IMAGE AREA
DROPPED HEAD; BEGIN SECTIONS HERE

Union Carbide personnel indicated that the potential for carbon fibers in furnace exhaust gases is minimal, because carbonization occurs in a controlled nitrogen atmosphere and the minimal quantity of off gases is controlled by a catalytic incinerator used because of cyanide by-products. Ventilation of certain areas of a production facility may emit carbon fibers, especially where the fibers are rewound and chopped into mats.

Union Carbide (Parma, Ohio) provided the following written information: they have "two potential emission sources associated with the production of carbon fibers. Source one is a production line for carbon mat fibers immediately following the carbonizing process. Source two is the exhaust system for a work area where carbon mat fibers receive additional processing.

"Source One: This source has an exhaust volume of 15,000 cubic feet per minute. At an approximate velocity of 3,000 feet per minute the air is exhausted at ambient temperatures. Prior to discharge into the atmosphere, the exhaust passes through the rotary drum filter to remove fibers."

"Source Two: This source has a discharge of 8,000 cubic feet per minute at the approximate velocity of 1,200 feet per minute. This source is also at ambient temperature. Prior to discharging into the atmosphere, this exhaust passes through a rotary drum filter, followed by a bag filter to remove carbon fibers and dust."

As a result of the survey undertaken within this program it has become apparent that the routine emission by manufacturing operations, of significant amounts of carbon fibers into the atmosphere is rather unlikely. It appears quite probable that the only environmentally detrimental releases of such fibers are to be associated with large scale, high temperature, possibly explosive, open incineration of carbon fiber composite materials, such as those studied by NASA.

Future drastic increases in the volumes of production of both fibers and their composites may, however, change this picture, as different methods of production are applied and as economic considerations may affect the degree and effectiveness of emission control measures. At this time and in the view of manufacturers of these materials, routine incineration of scrap composites and/or fibers is unusual because of the high cost of these materials which dictates minimization of waste and its disposal.

BEGIN LAST LINE OF TEXT HERE
BOTTOM OF IMAGE AREA OUTSIDE DIMENSION FOR TABLES AND ILLUSTRATIONS
3/8"

EPA-287 (Cin.)
(4-76)

BEGIN FIRST LINE OF TEXT HERE
TYPING GUIDE SHEET
CENTER OF PAGE
TOP OF IMAGE AREA
DROPPED HEAD: BEGIN SECTIONS HERE

SECTION 4

CARBON FIBER SAMPLING AERODYNAMICS

This discussion treats the transport properties as well as the dynamic behavior of carbon fibers with respect to sampling and flow ducting within a monitoring device. Fiber gravitational settling and inertial properties must be known in order to design the flow elements of a fiber monitoring instrument.

A relevant treatment of fiber aerodynamics has been presented previously within the context of the Fibrous Aerosol Monitor (FAM) prototype development, based on the original analysis by Fuchs. The dynamics of fibers are modeled by the behavior of ellipsoids of revolution with their axis either parallel or perpendicular to the direction of motion.

The equations from which the equivalent aerodynamic diameter can be obtained for fibers with various dimensions are, for the parallel axis-to-motion case:

$$D = \frac{4/3\ d}{\frac{2\beta^2 - 1}{(\beta^2 - 1)}\ \text{arc cosh}\ (\beta) + \frac{\beta}{\beta^2 - 1}} \qquad (1)$$

and for the perpendicular axis-to-motion case:

$$D = \frac{8/3\ L}{\frac{2 - 3\beta^{-2}}{(1 - \beta^{-2})^{3/2}}\ \text{arc cosh}\ (\beta) + \frac{1}{1 - \beta^{-2}}} \qquad (2)$$

where D is the diameter of the sphere having the same settling velocity, d is fiber diameter, L is the fiber length and β is the length-to-diameter ratio.

To determine the gravitational settling velocity for a given fiber, once the value of D has been determined, and provided that the particles fall vertically (no lateral glide) and do not change their orientation during their vertical motion, D can be replaced in the classical Stokes equation for the diameter of a spherical particle:

$$V_s = \frac{M_p - M_g\ g}{3\pi\ \mu D} \qquad (3)$$

BEGIN LAST LINE OF TEXT HERE
BOTTOM OF IMAGE AREA, OUTSIDE DIMENSION FOR TABLES AND ILLUSTRATIONS
3/8"

EPA-287 (Cin.)
(4-78)

BEGIN FIRST LINE OF TEXT HERE
TYPING GUIDE SHEET
CENTER OF PAGE
TOP OF IMAGE AREA
DROPPED HEAD: BEGIN SECTIONS HERE

where V_s is the settling velocity

M_p and M_g are the masses of the particle and the displaced gas, respectively (M_g is usually negligible)

g is the acceleration of gravity

μ is the coefficient of gas viscosity

The gravitational settling of graphite fibers (ρ = 2.25 g/m^3), as a function of length and diameter, has been plotted in Figure 1 for the two extreme fiber attitudes, based on Equations (1), (2), and (3). It is interesting to observe that the sedimentation velocity of such fibers is very insensitive to their length; e.g., for a horizontally falling 5 μm diameter fiber, the settling velocity varies from about 0.8 to 1.17 cm/sec for lengths ranging from 100 μm to 1 cm.

Even long fibers (L > 10 μm) falling with their axis vertical, settle only about 70 to 80 percent faster than those with their axis horizontal. Fiber diameter to a large extent determines sedimentation velocity. Thus the carbon fibers of interest having diameters of typically 5 to 10 μm settle with velocities of the order of 0.5 to 10 cm/sec depending on diameter, length and attitude.

Another aspect to be considered in the context of the aerodynamic behavior of fibrous-shaped particles is their orientation within a flow field as a result of shear forces exerted by the moving fluid. Although an acicular particle (rigorously an ellipsoid) tends to fall without rotation in a gravitational field, in the case of laminar flow through a duct, these particles tend to align with their long axis with the direction of flow. This is a result of the transverse velocity gradient in a fully developed laminar flow (i.e., with a parabolic velocity profile) which causes a torque on the elongated particle until alignment with the direction of flow is attained.

Carbon fibers with typical diameters ranging from about 2 to 15 μm, and lengths from about 10 to 10,000 μm, will behave inertially and aerodynamically similarly to unit density spheres of approximately 5 to 80 μm in diameter. This can be derived from Figure 1 which is a graph of calculated gravitational settling velocities in air for carbon fibers as a function of both fiber length and diameter (based on Fuchs' model of ellipsoids of revolution).[1]

Representative sampling of aerosol particles whose equivalent aerodynamic diameter is in the above determined range presents a challenge to the designer of monitoring instrumentation.

Two major aspects must be considered in this context:

(a) nonrepresentative sampling from a stream due to anisokineticity, and

(b) sampling line losses..

Both of these factors affect adversely the accuracy of any particle monitoring system, especially for the range of aerodynamic sizes under consideration.

BEGIN LAST LINE OF TEXT HERE
TOM OF GE AREA
OUTSIDE DIMENSION FOR TABLES AND ILLUSTRATIONS
3/8"

PAGE NUMBER
EPA-257 (Cont.)
(4-76)

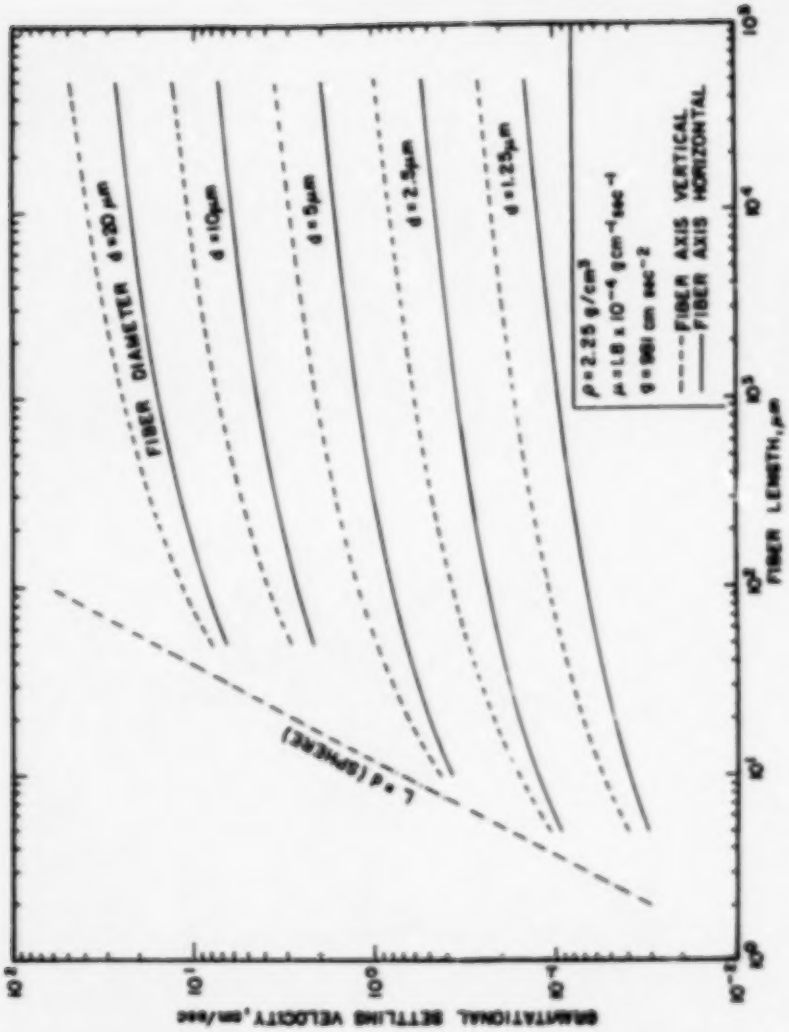

Figure 1. Gravitational settling velocity of graphite fibers as function of fiber diameter and length.

Isokinetic sampling is mandatory for any carbon fiber source monitoring instrumentation, with high flow rate sample extraction, because of the exceedingly long lengths of some of these fibers, which necessitates large inlet diameters to prevent interception and/or fiber breakup. Isokinetic sampling is usually straightforward except in those cases where inertial particle collection and sizing are required; e.g., in-stack cascade impactors, whose flow rate must remain constant.

Figure 2 is a plot of the particle concentration in the sample stream with respect to that of the main stream, as a function of the ratio of main stream-to-sample stream inlet velocity, for several unit density sphere diameters (in μm).[5] For particles with equivalent diameters of up to about 80 μm, and in order to limit sampling nonrepresentativeness to less than 10 percent, the above-mentioned ratio of velocities must remain within about 94 and 114 percent, a rather stringent requirement, best achieved by automatic (feedback) flow control.

Line losses are usually a serious problem for large particles; i.e., those exceeding aerodynamic diameters of about 10 μm. Probe bends must be avoided, if at all possible, and the length of horizontal runs must be minimized. Gravitational and turbulent wall deposition can affect seriously the results of aerosol measurements under these conditions, and these effects have limited the use of automated particulate monitoring instrumentation for stack emissions.

In the case of effluents from carbon fiber-related operations, the cross-sectional dimensions of ducts and stacks are, in most cases, small (i.e., on the order of 1 m in diameter, or less), thus reducing the probe lengths required to extract a sample.

In order to minimize inertial particle losses at the 90° bends of such probes, specially shaped probes such as the one depicted in Figure 3 can be used. The duct expansion at the bend results in a reduction of the extracted stream velocity thus reducing the centrifugal force component, at the same time that the larger outer radius provides a smoother transition to the new direction. Although for a bent pipe of constant cross section, the losses are independent of the bend radius,[6] losses decrease for an expanded bend (e.g., as shown in Figure 3).

The two-dimensional centrifugal inertial losses, E_c, at a bend are given by:[6]

$$E_c = S_t\, \theta/2 \qquad (4)$$

where θ is the bend angle (e.g., $\pi/2$ for 90°) and S_t is the Stokes number defined as:

$$S_t = \rho_p\, d^2 v/18\ \mu a \qquad (5)$$

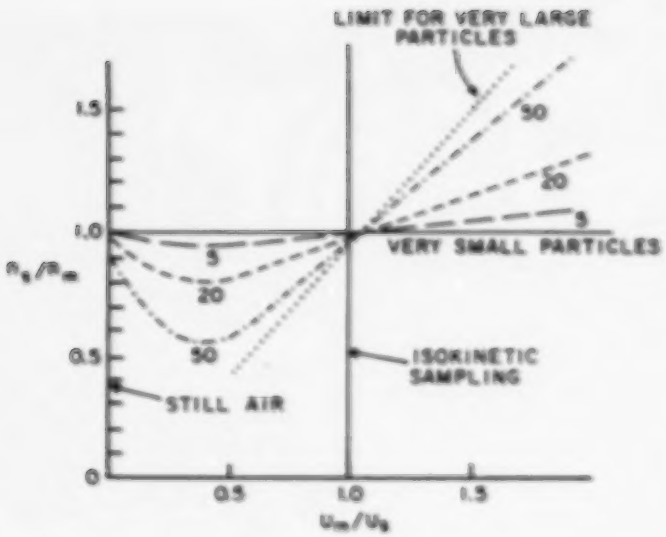

Figure 2. Effect of velocity ratio on concentration ratio for a sampling tube oriented in the direction of the mainstream flow. The curves are approximate representations of the data of various experimenters for unit density particles of diameters (in μm) as indicated. The displacement of the point $n_s/n_m = 1$ from $U_m/U_s = 1$ results from the finite particle diameter. The curves apply to a nozzle of 1 to 2 cm diameter sampling at about 5 m/sec.

BEGIN FIRST LINE OF TEXT HERE
TYPING GUIDE SHEET
CENTER OF PAGE
TOP OF IMAGE AREA
DROPPED HEAD. BEGIN SECTIONS HERE

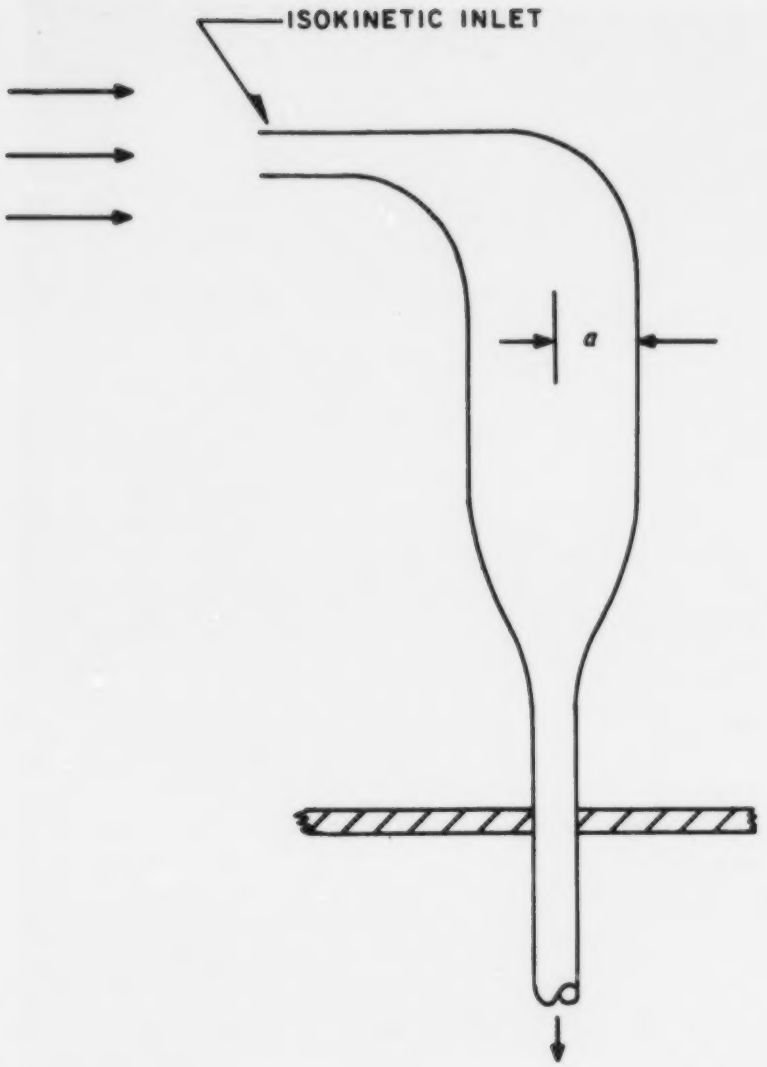

Figure 3. Expanded 90° probe bend designed to minimize inertial particle losses.

BEGIN LAST LINE OF TEXT
BOTTOM OF IMAGE AREA. OUTSIDE DIMENSION FOR TABLES AND ILLUSTRATIONS
3/8"

PAGE NUMBER
EPA-287 (Cin.)
(4-76)

BEGIN FIRST LINE OF TEXT HERE
TYPING GUIDE SHEET
CENTER OF PAGE
TOP OF IMAGE AREA
DROPPED HEAD; BEGIN SECTIONS HERE

where ρ_p is the particle density

d is the particle diameter

v is the stream velocity

μ is the coefficient of viscosity of the gas

a is the duct inner radius

For $\theta = \Pi/2$ (90° bend), Equation (4) is applicable for Stokes numbers less than $4/\Pi$ (for larger values of S_t the losses are always 100 percent).

For an expanded cross-section bend, as shown in Figure 3, the particle losses are decreased because v is decreased, and a is increased at the same time.

As an example of the above, at ambient temperature, for a stream velocity of 2 m sec^{-1} (approximately 400 feet/min), a sampling entrance nozzle diameter of 1 cm, an aerodynamic particle diameter (unit density sphere) of 40 μm, and for losses of less than 10 percent, the probe diameter at the bend must be increased to 2.5 cm. To achieve the same transmission efficiency for 80 μm unit-density spheres (i.e., the upper end of the carbon fiber equivalent size spectrum), the bend inner diameter would have to be increased to about 4 cm.

The preceding example implies a flow rate of about 10 liters/min which is a practical value for a typical monitoring instrument.

As mentioned before, horizontal probe lengths must be minimized for the particle sizes under consideration. Gravitational settling losses can be very significant for unit density equivalent spheres of the order of 80 μm in diameter. For the above case, assuming an unexpanded probe diameter of 1 cm, any horizontal lengths in excess of a few centimeters would result in relatively high gravitational deposition losses. Higher flow rates, accompanied by larger duct diameters would be required if longer horizontal runs are necessary. The overall monitoring system, however, should be designed around a vertical extraction flow axis; i.e., ducting to the outside of the stream, and sensing should be performed with vertical flows to minimize measurement errors caused by particle settling losses.

As a practical guide for the design of ducts and probes required to transport the sampled flow stream from its inlet to the monitoring device (assuming that such an extractive approach is used), a nomograph was designed which relates probe flow velocity, fiber sedimentation velocity, probe inner radius, probe length, with the resulting transport losses. This nomograph is shown in Figure 4. The dashed lines represent the steps to be followed for a specific example: flow velocity Vf = 5 m/s, settling velocity V_s = 0.012 m/s (corresponding to a sphere of 20 μm equivalent aerodynamic diameter), probe radius R = 0.02 m, and probe length L = 1 m.

The settling velocity for a carbon fiber of given length and diameter is obtained from Figure 1 or from Equations (1), (2), and (3). The nomograph of Figure 4 for the above assumed parameters, indicates that the exit

BEGIN LAST LINE OF TEXT
BOTTOM OF IMAGE AREA; OUTSIDE DIMENSION FOR TABLES AND ILLUSTRATIONS
3/8"

EPA-287 (Cin.)
(4-76)

BEGIN FIRST LINE OF TEXT HERE
TYPING GUIDE SHEET
CENTER OF PAGE
TOP OF IMAGE AREA
DROPPED HEAD; BEGIN SECTIONS HERE

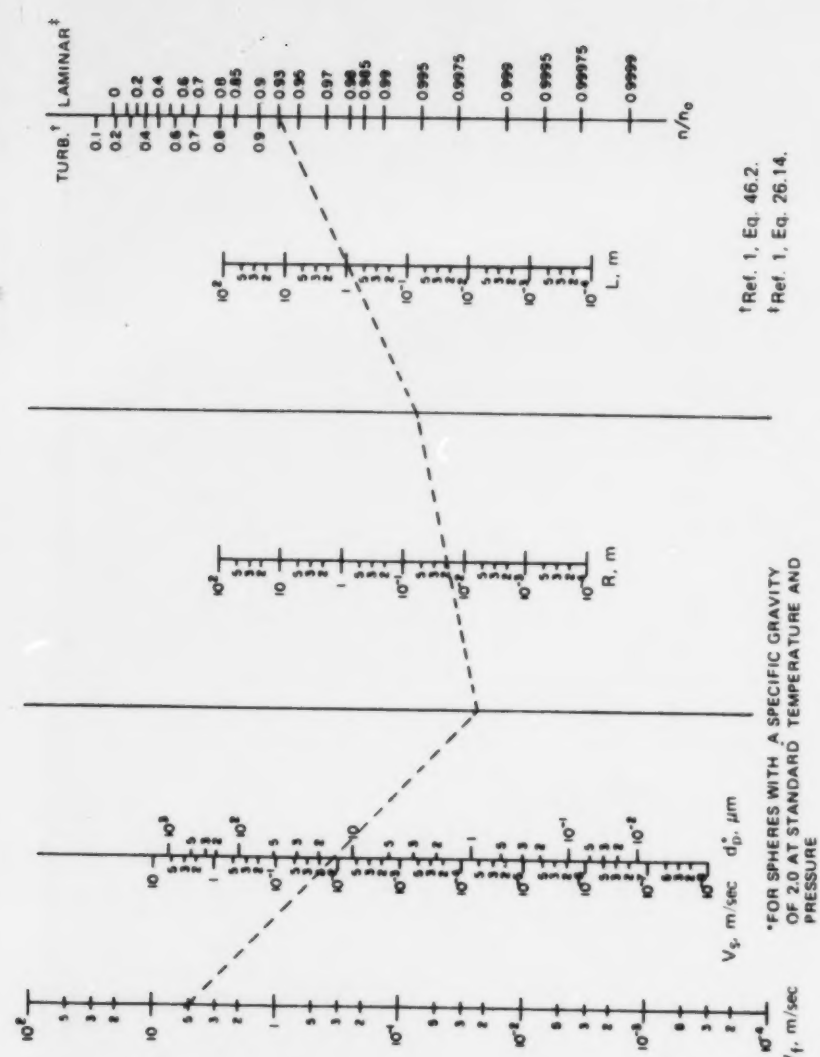

Figure 4. Nomograph for estimating gravitational settling losses in horizontal cylindrical ducts.

BEGIN LAST LINE OF TEXT
BOTTOM OF IMAGE AREA, OUTSIDE DIMENSION FOR TABLES AND ILLUSTRATIONS
3/8"

EPA-287 (Cin.)
(4-75)

BEGIN FIRST LINE OF TEXT HERE
TYPING GUIDE SHEET
CENTER OF PAGE
TOP OF IMAGE AREA

concentration of the probe would be 93 percent of the inlet concentration ($n/n_o = 0.93$); i.e., a loss of 7 percent which, in most cases, would be acceptable.

DROPPED HEAD; BEGIN SECTIONS HERE
6 1/2"
9 1/8"
BEGIN LAST LINE OF TEXT
BOTTOM OF IMAGE AREA; OUTSIDE DIMENSION FOR TABLES AND ILLUSTRATIONS
3/8"

EPA-287 (Cin.)
(4-76)

BEGIN FIRST LINE OF TEXT HERE
TYPING GUIDE SHEET
CENTER OF PAGE
TOP OF IMAGE AREA
DROPPED HEAD; BEGIN SECTIONS HERE

SECTION 5

METHODS OF CARBON FIBER DETECTION AND MONITORING

The discussion that follows is a description of the methods and techniques that are either available or potentially applicable for the monitoring of carbon fibers within stack and duct effluents that were uncovered in the literature search.

HIGH VOLTAGE SPARK SYSTEM

The first detection system to be discussed is the High Voltage Spark Carbon Fiber Detection System developed by the Jet Propulsion Laboratory. This detection method is based on the ability of a carbon fiber to initiate spark discharge across a high voltage-biased grid, from which counting and sizing of fibers can be derived.

Carbon fibers released from the combustion of carbon fiber composites may be coated with epoxy resin residues. In most cases, unprocessed raw carbon fibers are also precoated. Therefore, there is considerable difficulty in establishing electrical contact between a fiber and an electrode. Careful tests have shown that, in most cases, a carbon fiber laid carefully across a pair of electrodes shows no electrical conductivity if the bias voltage between the electrodes is less than 400 V. Beyond 400-500V of bias voltage, arcing starts to occur at the contact points so that there is electrical conduction through the fiber. Therefore, the reliability of a grid carbon fiber counting system is higher when using a high voltage bias than when using a low voltage bias.

Because of the relatively high resistance of the fiber, under a moderate high voltage bias (0.5 kV to 2.0 kV), a carbon fiber draws only a very small current between a pair of grid electrodes. It can be heated red hot, but rapid burnout does not readily occur. Thus, most problems associated with a low voltage biased grid fiber detector remain under high bias voltage; that is, the decrease of sensitivity as fibers accumulate on the grid, and the creation of multiple irregular signals as a single fiber bounces around the electrodes of the grid. To quickly burn out a fiber by electrical heating takes considerable electrical power and may be impractical.

JPL's concept was to achieve individual fiber counting by using a pulse discharge technique which is schematically shown in Figure 5. The electrical energy is stored in a small capacitor C. The high voltage leads of the capacitor are directly connected to the grid wherein alternate electrodes of the grid are biased positively and negatively. Upon conductivity being

BEGIN LAST LINE OF TEXT
BOTTOM OF IMAGE AREA; OUTSIDE DIMENSION FOR TABLES AND ILLUSTRATIONS
3/8"

EPA-287 (Cin.)
(4-76)

BEGIN FIRST LINE OF TEXT HERE
TYPING GUIDE SHEET
CENTER OF PAGE
TOP OF IMAGE AREA
DROPPED HEAD: BEGIN SECTIONS HERE

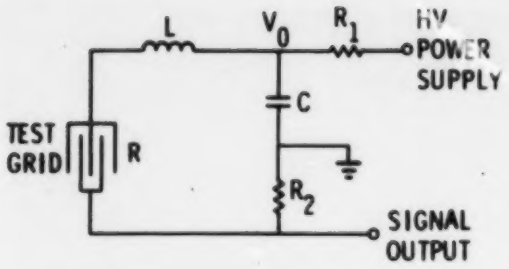

$R^2 > \frac{4L}{C}$ EXPONENTIAL

$R^2 = \frac{4L}{C}$ CRITICAL DAMPED

$R^2 < \frac{4L}{C}$ OSCILLATORY

R_1 • CURRENT LIMITING RESISTOR
$\simeq$ 1 kΩ

R_2 • CURRENT SHUNT
$\simeq$ 0.005 TO 0.1 Ω

C $\simeq$ 0.05 μF

L • CIRCUIT INDUCTANCE
$\simeq$ 0.5 μH

R • SPARK RESISTANCE
$\simeq$ 0.5-10 Ω

NOTE: R IS VOLTAGE DEPENDENT

Figure 5. Spark discharge circuit schematic diagram.

BEGIN LAST LINE OF TEXT
BOTTOM OF IMAGE AREA OUTSIDE DIMENSION FOR TABLES AND ILLUSTRATIONS
3/8"

EPA-287 (Cin.)
(4-76)

established by a carbon fiber, a discharge phenomenon occurs in a typical manner of an RLC circuit. The inductance L comes from the self-inductance of the grid lead wires. It can be minimized by shortening the lead wires but it cannot be completely eliminated. The value of the inductance L with about 7.6 cm (3 in.) long lead wires was about 0.5 μh.

A typical discharge current waveform is shown in the Figure 6. By using this approach, a number of advantages are apparent:

1) The signals for fiber counts are prominent and reproducible.

2) The short duration of the signal, 0.5 to 1.0 μs, is favorable for high counting rate operation. In fact, this rate is mainly limited by the recharging time of the capacitor C.

3) The contact resistance problem is eliminated by the high voltage.

4) The grid is self-cleaning, i.e., fibers do not accumulate on the grid. Therefore the problem of decrease in sensitivity due to more than one fiber across the grid electrodes is eliminated. Also, since the fiber does not stay long on the grid, repetitive irregular arc signals produced by a single fiber are avoided.

5) There is strong evidence indicating that the use of a high voltage bias increases the fiber counting efficiency. The fiber fragments, being conductors, polarize under an electrical field and thus are attracted to the grid.

Under a moderately high voltage, the electrical field is strong enough to overcome the air flow pattern. It aligns the fiber perpendicularly to the axis of the electrodes (grid) and the plane of the grid. Therefore the probability of fiber contact is enhanced, ensuring the generation of a spark count. In the absence of the electrical field, the fiber fragments presumably will align with the stream lines of the air flow which is parallel to the axis of the grid plane. One can envision, in this case, that it is easy for fibers to flow through the grid without contacting the grid electrodes.

The JPL high voltage (H.V.) spark carbon fiber detection system was developed to monitor carbon fiber fragments in the length range of 1 to 5 mm. It consists of the following sub-assemblies:

1) A grid-windbox assembly which contains:

   a) A grid made of a number of equally spaced, parallel copper blade electrodes secured in a frame made from electrically insulated material. The electrodes are biased by a high voltage circuit.

   b) A pre-screen (a stainless-steel screen with square meshes) to prevent fiber clusters from short-circuiting the grid-bias circuitry.

BEGIN FIRST LINE OF TEXT HERE
TYPING GUIDE SHEET
CENTER OF PAGE
TOP OF IMAGE AREA
DROPPED HEAD: BEGIN SECTION HERE

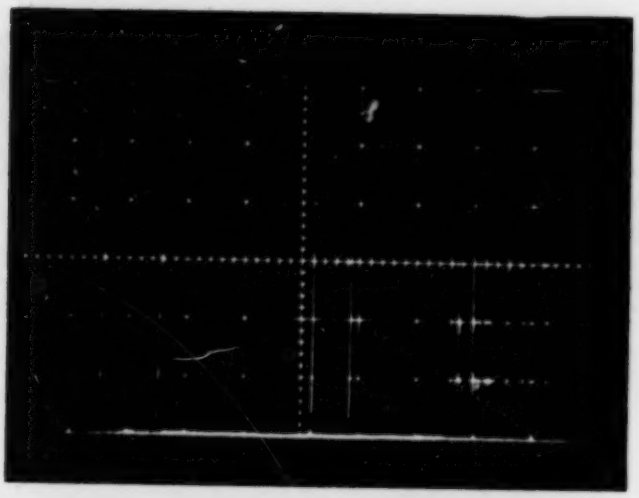

2 V/DIV
5 s/DIV
V_0 = 1 kV
GRID SPACING ≈ 4 mm

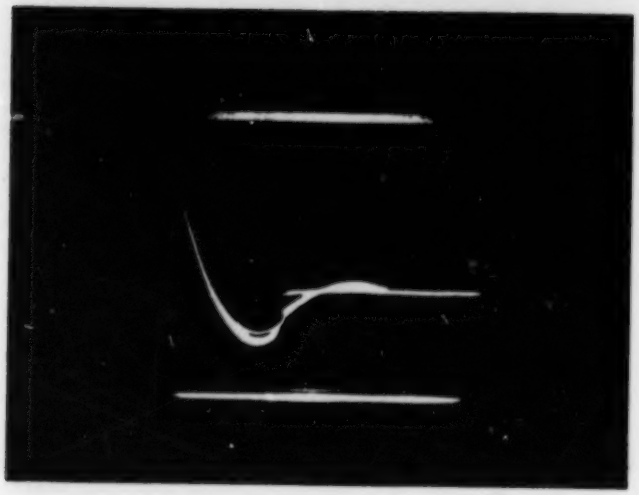

1 V/DIV
0.2 μs/DIV
V_0 = 1 kV
GRID SPACING ≈ 7.5 mm

Figure 6. Typical discharge current waveform as recorded by an oscilloscope.

BEGIN LAST LINE OF TEXT
3/8"
BOTTOM OF IMAGE AREA; OUTSIDE DIMENSION FOR TABLES AND ILLUSTRATIONS

EPA-287 (Cin.)
(4-76)

c) An AC voltage-driven fan.

d) A windbox, which works in conjunction with the fan to sample the air.

3) High voltage discharge circuit to store electrical energy and provide the high voltage bias for the grid. It sends out a prominent pulse signal, which is subsequently counted when the spark is initiated by a fiber in contact with the grid.

2) A pulse integrator electronic package. This unit provides the pulse-shaping function for the input spark signal and integrates these pulses so that a DC voltage output is provided which corresponds to the total number of fiber counts; this signal is registered on a strip chart recorder.

The following lists the general specifications for the system:

1) Fiber length detection ranges: 1-2 mm, 2-3 mm, 3-4 mm, 4-5 mm, 5-10 mm.

2) Counting rate = $I/CV = 6.6 \times 10^3 \frac{I}{V}$

where I = H.V. power supply current in mA

V = H.V. power supply voltage in volts

C = Capacitance of the discharge capacitor in farads

= 0.14 μF

3) H.V. pulse discharge circuitry

Capacitor bank = 0.14 μF

Current limiting resistor = 1 W 1 KΩ

Signal output amplitude = ~-5 V

Signal output duration = ~0.5 μs

4) Nominal operation AC voltage for fans = 50 V rms

5) Pulse integrator

DC input = 40 V

Signal input = -5 V nominal

Signal output 10 ns to 5 μs rise time
= 0 to -10 V, automatically reset at -10 V

Sensitivity = ~10 pulse/volt

BEGIN FIRST LINE OF TEXT HERE
TYPING GUIDE SHEET
CENTER OF PAGE
TOP OF IMAGE AREA
DROPPED HEAD: BEGIN SECTIONS HERE

6) Mechanical

Grid-windbox assembly = 10.7 x 12.1 x 17.0 cm
1.3 kg

Pulse integrator = 5.1 x 12.7 x 17.8 cm
0.39 kg

7) Other relevant physical parameters (see Table 2)

TABLE 2. RELEVANT PHYSICAL AND OPERATIONAL PARAMETERS OF SPARK SYSTEM

CHANNEL NO.	1	2	3	4	5
Grid gap, mm	1.19	2.38	3.58	4.477	5.97
Bias Voltage, Volts	510	690	870	1020	1200
Threshold Fiber Length, mm	1.0	2.0	3.0	4.0	5.0
Prescreen Mesh Size, mm	1.50	2.44	3.43	4.69	5.46
A, Total Aperture x 10^{-3} m^2	4.80	4.80	5.0	5.56	5.36
V, Wind Speed at 50 V Variac, m/s	1.40	1.52	1.78	1.98	2.41

BRASS BALL TECHNIQUE

The following is a brief discussion of the instruments and techniques used or explored in the NASA "Carbon Fiber Risk Analysis" program.[8] The instruments fall into the two categories of active and passive methods. The instruments are inserted into an air stream which carries the carbon fiber fragments from the source of fiber, i.e., a burning carbon fiber composite. The active instruments can provide a direct signal to indicate the relevant information on the fiber concentration and length distribution, while the passive instruments can collect the fibers for post-test examination and analysis.

The instruments for monitoring these fibers were developed for optimized performance in the 1 to 4 mm fiber length region. The fiber density dealt with in these studies was relatively low due to very limited amounts of carbon fiber composites that were tested and the large distance between the fiber release source and the sensing device.

BEGIN LAST LINE OF TEXT
BOTTOM OF IMAGE AREA OUTSIDE DIMENSION FOR TABLES AND ILLUSTRATIONS
3/8"

EPA-297 (Cln.)
(4-76)

When small airborne conducting particles and fibrils strike a conducting surface with an electric charge distribution on it, they acquire charge and are repelled from the surface. If the conducting surface is connected to a power supply of constant potential, a charging pulse is observed as each particle or fibril makes contact with the surface. A collection of such charging pulses can be processed by a pulse height analyzer to yield information about the size and frequency of conducting airborne particles.

The brass ball technique was developed by the U.S. Army at Aberdeen Proving Grounds. It consists of a 3.8 cm (1.5 in) diameter brass ball supported by a plastic insulated Rod-electrode. The ball is charged by a high voltage power supply to about 1 kV through a high-impedance current limiting resistor, and it is connected in parallel to a small capacitor. The ball thus attracts the fiber fragments, in a flow stream. Upon contact with the fiber, the capacitance of the ball is changed, thereby generating an electrical signal. Experience has shown that the amplitude of this signal is correlatable to the fiber length. The disadvantages of the system are:

a) The signal is weak, in the millivolts range, therefore requiring amplification by sophisticated electronics. The equipment required for such amplification and signal processing limits portability for field tests.

b) The detection system is intrinsically noisy thereby impeding the detection of short fiber fragments with lengths below 2 mm.

c) The fiber capture efficiency of the device is low and dependent upon the velocity of the surrounding air stream.

d) The system is sensitive to moisture and soot.

These problems make the system relatively inconvenient for field tests and for many laboratories.

LOW VOLTAGE GRID SYSTEM

This approach was explored at JPL in the early stages of the fiber gasification development program. It was soon abandoned due to a variety of problems. The system used parallel brass-rod grids supported in an insulated frame. The adjacent rods were biased by low voltage DC up to 15 volts. When a fiber was collected in the grid, it drew electrical current, thereby producing an electrical signal. The most serious problems encountered within this device were:

a) Loss of sensitivity due to fiber accumulation on the grid.

b) Multiple irregular signals produced when a single fiber made multiple contacts with the grid.

c) Low count efficiency due to: 1) fibers passing through grid, and a) the variable high value of contact resistances which existed between the fiber and brass-rod electrodes.

The attractive features of the system were its simplicity and the safety of operation because of the low bias voltage used.

CONTINUOUS OPTICAL COUNTER

A light source such as a LED or laser beam is incident on a photodiode device. When the air flow carrying the fiber fragments passes between these two elements the shadow of the fiber generates an electrical signal. The major advantage of the system is its high counting rate capability. It has several serious problems when applied to fiber monitoring.

a) It cannot differentiate fibers from the soot in the flame or dust particles in the air.

b) The signal response (pulse shape) as well as sensitivity are very dependent on the flow rate and optical design.

c) Fiber length is not easily determined.

LIDAR

This system detects the back scattering of a laser beam by the fibers (or any other particulates), and is in principle similar to a RADAR. The sensitivity attainable with the system probably limits its application to a dense cloud of fibers. Even in that case, the noise generated by the soot also poses a serious problem, i.e., this method is non-fiber specific.

MICROWAVE

This technique is being pioneered by TRW Systems, Inc., under the sponsorship of NASA and USAF, and currently technical details are not available. It is believed to be based upon a common microwave approach, and the system presumably uses a microwave waveguide. The fibers flowing in the air across the waveguide will attenuate the transmission and induce reflections of the electromagnetic waves propagating in the guide. By monitoring these parameters, gross fiber concentration information could be obtained. Thus, the technique cannot measure the length of individual fibers, and the sensitivity is questionable because the cross-section of a microwave waveguide cannot be made arbitrarily small.

STICKY TAPE

The sticky tape and the filter techniques (see next section) are examples of passive methods. The sticky tape is a convenient and economical means of collecting fiber fragments and storing fiber information. It is worthy of mention because so far it is the most frequently used technique in field tests. Needless to say, fiber counting under an optical microscope is a very tedious procedure and therefore limits its effectiveness. Two automated readout techniques, both being investigated at JPL, may bring a solution to this problem.

The first one uses photographic film and a microdensitometer to digitize the fiber image and subsequently process it by a digital computer system. The second technique for counting the fibers collected on the sticky tape, which to date is a very promising one, uses a set of high voltage plate electrodes (similar to the high voltage grid technique). Under a proper high voltage bias, the device generates sparks as guided by the fibers collected on the tape when the tape is in contact with the electrodes. The spark destroys the fiber and generates an electrical signal. In this way, high counting rate of the fibers previously collected on the tape can be accomplished.

So far, there is no reliable calibration data for the tape method. The accurate interpretation of the sticky tape data, just as for any other fiber detection instrument, is dependent on a variety of parameters such as air flow rate, angle of incidence, shape of the tape, temperature, soot interference, etc. Recently, preliminary tests at JPL have shown the capture efficiency of the tape to be quite poor. The efficiency ranged between 5% and 10% for a nominal wind speed of 0.5 to 2.0 m/s.

FILTER TECHNIQUE

In the NASA field tests,[8] bridal veil screens of different mesh were used in a variety of geometrical configurations to collect fibers. This is a most effective way to collect fiber clusters. For a single fiber fragment the fiber capture efficiency is uncertain.

The above discussed group of techniques summarizes those developed and applied under the NASA "Carbon Fiber Risk Analysis"[8] program aluded to previously. Additional candidate methods and techniques applicable to the carbon fiber monitoring problem are presented in the following sections. Major emphasis will be placed on the photo-thermal technique conceived within this program at CCA.

SPECTROPHONE

The spectrophone provides a new way to monitor atmospheric aerosols. Different information is obtained from absorption measurements than from scattering measurements because dependence on particle size distributions and optical properties of the aerosols are different. The absorption by particles less than about 1 μm in diameter would, in the first approximation be proportional to their total volume, independent of their size distribution. This constrasts sharply with the scattering of a given volume of small particles. A major advantage of the spectrophone is its insensitivity to scattered light.

The spectrophone operates on the principle of detecting sound waves generated by localized time-dependent heating of the air. In the case of absorption of light by aerosols, sound generation in the spectrophone is limited by the rate at which the heat is transferred to the gas from the particles.

Experiments have been performed to monitor the mass of carbonaceous aerosols with a spectrophone.[9] In this particular experiment a helium-cadmium laser with a measured output of 3 mW at 4166 Å was used. The laser beam is chopped at 4000 Hz to power an accoustically resonant spectrophone. The modulated heating of particles at 4000 Hz is efficient in generating sound for particles up to about 3 μm in diameter. This method is obviously specific to carbon but not to particle shape; i.e., fibers cannot be distinguished from other shaped particles. This general principle, however, will be further elaborated within the description of the photo-thermal technique, further on within this section.

THE MICRO-RAMAN TECHNIQUE

The Laser-Raman microprobe developed at the NBS is employed in the spectroscopic characterization of carbonaceous matter associated with air pollution particulate samples.[10]

Detection and measurement in the Raman microprobe are based on the observation of the normal or spontaneous Raman effect. This effect provides the basis for Raman spectroscopy. In the Raman measurement, a beam of monochromatic, visible laser light is focused on the sample. The radiation scattered by the sample contains weak lines, at frequencies both lower and higher than the existing radiation. The frequency differences, (with respect to that of the illuminating beam) called Raman shifts, are characteristic of the sample material and are independent of the exciting frequency. The spectra obtained with the Raman microprobe are the so called Stokes-Raman spectra. They arise from molecules which scatter photons of lower frequency (Stokes lines) than that of the exciting line. The Raman pattern they represent provides a molecular fingerprint for identification and characterization. The spectrum is usually excited in a region where the sample does not absorb. Appreciable absorption of the exciting radiation generally leads to sample heating, frequently attended by sample modification or destruction. In microprobe measurements, such problems can be particularly severe because of the high irradiances (power/unit area) that must be employed to excite analytically useful spectra. A major potential limitation in all Raman work is sample fluorescence which may totally swamp the Raman effect. With a choice of laser frequencies, problems of radiation absorption and sample fluorescence can often be minimized, if not virtually eliminated. Thus, it is often possible to select such an excitation frequency that color of a sample is not a limiting factor.

Identification and characterization of molecular species present as major components of microsamples are made by qualitative comparison with reference spectra. If these are not available in the literature from measurements on bulk samples, the information is obtained from microprobe measurements of well-characterized materials.

The instrument is a monochannel spectrometer. For excitation of the Raman spectrum, the light from an argon/krypton ion laser is focused to a small (typically 2-20 μm) spot on the sample. Nonlasing plasma lines are removed through the use of a predispersing prism. The light scattered by the sample

BEGIN FIRST LINE OF TEXT HERE
TYPING GUIDE SHEET
CENTER OF PAGE
TOP OF IMAGE AREA
DROPPED HEAD. BEGIN SECTIONS HERE

is collected by an ellipsoidal mirror in a 180° back-scattering geometry and transferred into a double monochromator equipped with concave holographic gratings. The signal is detected by a thermoelectrically cooled photomultiplier tube and processed by photon counting electronics. The sample is supported by a substrate (typically sapphire or lithium fluoride) mounted on a remotely-controlled sample stage. A built-in microscope allows viewing of the sample in transmitted light at magnifications up to 400 X. Irradiance levels employed in routine probe measurements range from several megawatts/cm^2 to several kilowatts/cm^2. Measurement times for solid microsamples of mass 10-100 pg may vary from 20 minutes for (fast) survey spectra to scans requiring 3-5 hours for radiation-sensitive materials.

For measurement in the Raman microprobe, the microsamples are usually supported by either a sapphire (α-Al_2O_3) or a lithium fluoride (LiF) substrate. Various methods of sample preparation used with this technique are available. Airborne particles are collected by conventional aerosol sampling techniques, consisting primarily of bulk sample collections on various types of filters and size-classified particle collections obtained through the use of multistage cascade impaction samplers.

Again, as in the case of the spectrophone, Raman scattering is limited to the identification of carbon in the aerosol particle sample, without providing fiber-shape discrimination.

OPTICAL ATTENUATION

A schematic of the apparatus developed for making optical attenuation measurements is shown in Figure 7. This attenuation measurement apparatus compares the transmission of a 633-nm He-Ne laser beam through a loaded filter relative to that of a blank filter.[10] The loaded filters are placed in the beam with the loaded side towards the laser; after multiple scattering through the filter substrate, the light is collected by an f/1 lens and focused on a photomultiplier tube. The optical attenuation measurement can be made with a wide variety of filter media. This technique is based on a principle similar to that of the opal glass method and measures the absorbing rather than the scattering properties of the aerosol. Since the real parts of the refractive indices of the filter media and the particulates are approximately equal, the addition of a few monolayers of nonabsorbing particles is expected to be a small perturbation on the transmission properties of the filter. This was verified for a Millipore filter loaded with 20 µg/cm of nonabsorbing 3-µm NH_4HSO_4 aerosols. Also, heat treatment and solvent extraction experiments have shown that one can remove from a filter substrate most of the mass of the aerosol responsible for scattering without appreciably affecting the optical attenuation. Therefore, the optical attenuation measured in the above fashion is attributed to the absorbing component in the aerosol. This method is also limited to the identification of carbon without particle shape characterization.

LIGHT SCATTERING METHODS

The light scattered by airborne fibers exhibits a very characteristic angular distribution very sharply confined to the plane perpendicular to the

BEGIN LAST LINE OF TEXT
BOTTOM OF IMAGE AREA, OUTSIDE DIMENSION FOR TABLES AND ILLUSTRATIONS
3/8"

EPA-287 (Cin.)
(4-76)

BEGIN FIRST LINE OF TEXT HERE
TYPING GUIDE SHEET
CENTER OF PAGE
TOP OF IMAGE AREA
DROPPED HEAD; BEGIN SECTIONS HERE

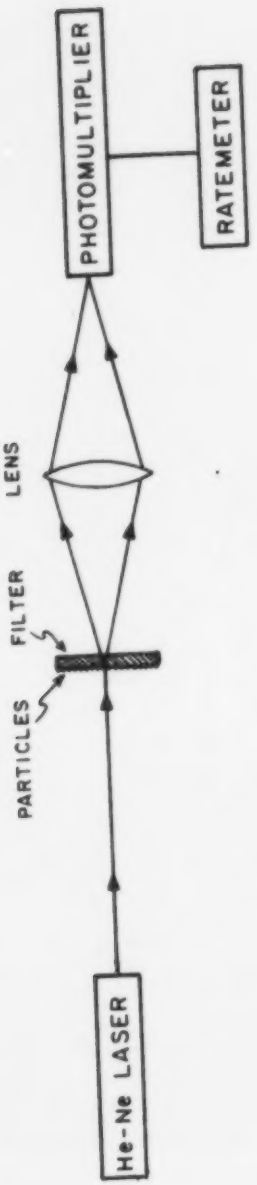

Figure 7. Schematic of the optical attenuation apparatus.

BEGIN LAST LINE OF TEXT
BOTTOM OF IMAGE AREA; OUTSIDE DIMENSION FOR TABLES AND ILLUSTRATIONS
3/8"

EPA-257 (Cin.)
(4-76)

BEGIN FIRST LINE OF TEXT HERE
TYPING GUIDE SHEET
CENTER OF PAGE
TOP OF IMAGE AREA
DROPPED HEAD. BEGIN SECTIONS HERE

fiber axis. Discriminatory fiber detection using this light scattering property can be effected by several sensing configurations: electric-field-induced rotation or oscillation combined with collimated illumination,[11-12] forward scattering diffraction pattern multiple detector sensing,[13] etc. Size; i.e., length, information can be obtained from these techniques by a detailed analysis of the light scattering angular dependence. This general approach can, and has been applied to the identification of fibers deposited on filters, with and without alignment by magnetic or by electric fields. A detailed description of the method of electric alignment and oscillation combined with light scattering detection will be presented further on.

LIGHT POLARIZATION

A population of fibrous-shaped particles, aligned by flow shear, electric or magnetic fields results in partial polarization of a light beam transversing such a cloud. The degree of polarization of the transmitted light, in combination with other complementing information (e.g., particle number concentration, etc.) can be used to characterize an aerosol containing acicular particles.

6-1/2"

DIFFERENTIAL CONDUCTIVITY SENSING

This technique is an extension of the Coulter-Counter particle sizing method modified to achieve a directed approach flow in order to align the fibrous-shaped particles within the conductive fluid, prior to their passage through the detection orifices.[14] This technique requires suspension of the airborne particles in the liquid medium, which must have a conductivity that is significantly different from the carbon fibers to be sensed.

The particle-in-liquid differential conductivity approach of the basic Coulter Counter described above can be extended to a similar configuration in air using a continuous glow discharge through a small detection orifice.[15]

DIFFERENTIAL ELECTRIC MOBILITY

Fibrous-shaped particles have been observed to exhibit clearly different electric mobility than isometric particles, permitting depositional segregational of such fibers in specially designed mobility analyzers.[16] The higher mobility exhibited by acicular particles appear to be caused by an enhancement of the electric charging process under a predominant diffusion charging regime in a corona discharge.

ELECTRIC ALIGNMENT OF FIBROUS-SHAPED PARTICLES

Elongated particles are aligned very easily in air for applied field intensities exceeding approximately 1,000 V/cm. Conductive fibers, such as carbon fibers whose typical resistance may be between 10 and 100 ohms, are aligned more rapidly than dielectric fibers.[11] Electric fiber alignment may be used either to orient these particles along a specific direction (by means of a d.c. field), or may be used to impart a controlled periodic motion (e.g.,

BEGIN LAST LINE OF TEXT
BOTTOM OF IMAGE AREA; OUTSIDE DIMENSION FOR TABLES AND ILLUSTRATIONS
3/8"

PAGE NUMBER
EPA-287 (Cin.) (4-76)

BEGIN FIRST LINE OF TEXT HERE
TYPING GUIDE SHEET
CENTER OF PAGE
TOP OF IMAGE AREA

rotation, oscillation, precession, etc.) to these elongated particles in order to effect detection by other means (see above).

DROPPED HEAD; BEGIN SECTIONS HERE

MAGNETIC ALIGNMENT OF FIBROUS-SHAPED PARTICLES

Acicular particles that exhibit paramagnetic or diamagnetic properties, when subjected to an externally applied magnetic field tend to align either with or perpendicularly to the magnetic field lines. Asbestos and graphite fibers have thus been aligned. This property may be used as means to discriminate between carbon fibers and certain other types of fibers.

Using the diamagnetic susceptibility of carbon, two pairs of Helmholtz coils can be used in the same manner as two pairs of electrodes to cause alignment and/or oscillatory motion of airborne carbon fibers. The magnetic field method would eliminate any electrode shorting problems; it would, however, require large fields and higher power consumption than the electrical counterpart. Magnetic fields can and have been applied to align filter-collected fibers.

AERODYNAMIC ALIGNMENT OF FIBERS

Acicular particles exhibit certain aerodynamic-inertial properties that are uniquely associated with their elongated shape. Settling velocities in a gravitational field, inertial behavior in flow fields of changing direction, positional response to shear flows, etc., differentiate such fibrous particles from isometric ones. Aerodynamic size of fibers is strongly dependent on their diameter while weakly influenced by their length. Fiber axis alignment along the flow direction occurs in laminar flow regimes due to the torque produced by the exclusively radial velocity gradient of such non-turbulent flows. This type of alignment can be used in conjunction with light scattering for the selective detection of fibers.

ULTRASONIC EFFECTS

A population of airborne fibers, especially if those are aligned by one of the above-mentioned methods, will influence the propagation of ultrasonic waves. Ultrasonic scattering and diffraction phenomena result when such waves interact with fibers whose dimensions are comparable to the sound wavelength. This technique has been applied to medical imaging and industrial analysis. Typical frequencies of the order of tens of MHz can be generated by means of magnetostrictive transducers. These ultrasonic beams, however, do not have the coherence and collimation of laser-generated light beams and cannot be focused as efficiently to achieve high power densities.

MICROSCOPY AND VIDEO ANALYSIS OF COLLECTED SAMPLES

This overall technique is used at present as a reference method to determine concentrations of such fibrous aerosols as asbestos. Filter collection followed by optical microscopy is the standard NIOSH method. A number of variations of this overall technique have and are being investigated: electron microscopy (TEM and SEM), video scanning image analysis, light scattering pattern analysis, etc.

BEGIN LAST LINE OF TEXT
BOTTOM OF IMAGE AREA, OUTSIDE DIMENSION FOR TABLES AND ILLUSTRATIONS
3/8"

EPA-287 (Cin.)
(4-76)

BEGIN FIRST LINE OF TEXT HERE
TYPING GUIDE SHEET
CENTER OF PAGE
TOP OF IMAGE AREA
DROPPED HEAD; BEGIN SECTIONS HERE

The filter collection-microscopy method would be used as the basic reference comparison technique for performance testing of any other fiber detection method.

The obvious disadvantages of this overall method applied to a stack and duct monitoring instrument is its off-line character, with typical time delays in information output ranging from a minimum of hours to typical periods of several days. Inaccuracy resulting from human interpretation errors (optical microscopy of filter samples), and/or as a result of the multiplicity of steps required to obtain the final information (aerosol sampling, collection, surface sampling, optical or electronic magnification, image interpretation, etc.) are another disadvantage of this overall approach.

SPARK DISCHARGE SPECTROMETRY

There exists a class of methods based on the detection and analysis of the electro-magnetic spectrum associated with electric discharges involving the material under scrutiny. Spark, arc, glow and corona discharges have been used; with alternating or with direct current excitation; in vacuum, in air and in pure carrier gases; with high-field, high current, or radioactive-source ionization; high-current density or laser-flashed surface vaporization, etc. Some of these will be treated separately in this listing.

The basic spark discharge spectrometry method to be considered in the present context consists of flashing individual carbon fibers by contact between and across high voltage electrodes (similar to the spark method discussed in a preceding section), in combination with the detection of the resulting light emissions spectrum, or of specific lines of such a spectrum for the identification of a particular element. There are several strong lines in the emission spectrum of the resulting carbon spark that uniquely characterize the presence of that element.

LASER FLASHING - SPARK SPECTROMETRY

This technique has been applied principally to surface analysis of materials; its application to the analysis of airborne carbon fibers should, however, be considered. The basic technique consists of the emission of a high energy, concentrated, short duration laser pulse aimed at the surface to be analyzed. A spark gap configuration near the laser target area is then triggered by the small plasma cloud generated by the laser pulse. The resulting emission lines in the electromagnetic spectrum are characteristic of the elements vaporized from the surface under scrutiny.

For the application under consideration here, the laser flash would be triggered by a preceding light scattering particle detection and identification as a fiber (see above), and by an appropriate time delay given by the flow velocity (laminar regime) and the distance between the light scattering detector site and the pulsed laser focus.

BEGIN LAST LINE OF TEXT HERE
BOTTOM OF IMAGE AREA, OUTSIDE DIMENSION FOR TABLES AND ILLUSTRATIONS
3/8"

EPA-287 (Cin.)
(4-76)

BEGIN FIRST LINE OF TEXT HERE
TYPING GUIDE SHEET
CENTER OF PAGE
TOP OF IMAGE AREA
DROPPED HEAD; BEGIN SECTIONS HERE

SCINTILLATING PARTICLE ANALYSIS

This technique has been applied, in a commercial instrument, to the identification of specified chemical components of individual airborne particles.[18,19] This method is based on the flame vaporization of discrete aerosol particles as they traverse a combustion chamber. Again, the resulting electromagnetic emission resulting from this controlled micro-combustion process is then detected, usually by means of one or more photodetectors with spectral filters centered on characteristic emission lines of the species of interest.

In the present context, this technique could be used to identify the predominance of carbon once a given particle has been characterized as being of fibrous shape.

X-RAY TECHNIQUES

The use of X-rays for the analysis of particulate composition has become rather common. These techniques, however, have always been applied to collected particle analysis; i.e., principally for the analysis of particulate deposition on filter substrates. X-ray diffraction is frequently used for the assessment of quartz (i.e., silica) in filter samples collected in coal mines and similar environments,[20] whereas X-ray fluorescence is a technique currently applied to the chemical analysis of samples collected in ambient and source environments.[21,22] The complexity of the required equipment has restricted the use of these methods to laboratory situations, and no concerted effort has been made to develop them into field-applicable instrumentation. Furthermore, both X-ray diffraction and fluorescence require substantial samples in order to provide an adequate signal, a constraint that may eliminate these approaches from providing a practical solution to the present problem.

DIFFERENTIAL LIGHT SCATTERING

Scattering of electromagnetic radiation by airborne particulates can, in some cases, be used to characterize the presence of specific predominant materials. This technique is based on the detection of characteristic differences in the index of refraction of particles illuminated at two or more differing wavelengths. Once a particle has been sized and characterized as a fiber by other means (e.g., alignment and single-wavelength angular scattering dependence) it is possible to determine the predominance of a specific material (e.g., carbon), by selecting two wavelengths for which this material exhibits largely differing indexes of refraction; i.e., one of which may be associated with specific infrared absorption lines or bands. This method may also be applicable in the microwave spectral region.

BEGIN LAST LINE OF TEXT HERE
BOTTOM OF IMAGE AREA, OUTSIDE DIMENSION FOR TABLES AND ILLUSTRATIONS
3/8"

EPA-297 (Cin.)
(4-76)

BEGIN FIRST LINE OF TEXT HERE
TYPING GUIDE SHEET
CENTER OF PAGE
TOP OF IMAGE AREA

The following two techniques, both originally conceived at GCA, one of which has been developed into a comercially available instrument (FAM-1), will be presented forthwith in considerable detail.

DROPPED HEAD; BEGIN SECTIONS HERE

FIBER DETECTION BY LISMEFA

Electric Field Fiber Alignment and Oscillation

Although the operating principles of the light scattering modulation by electric field fiber alignment and rotation (LISMEFA) technique, developed at GCA over the past 5 years, have been described in the literature,[11,12] its most important characteristics and its specific application to the present case of carbon-graphite fiber detection will be reviewed in this section. Furthermore, some of the operating and design approaches described in the above cited references (which applied to the original prototype instrument) have been superseded by recent advances which could be applied to the design of the carbon fiber monitoring system.

The LISMEFA technique is based on the following, essentially concurrent steps: (a) electrical polarization* of a fiber (i.e., elongated particle) by an applied electric field (d.c. for the FAM-1 second generation instrument), (b) alignment of the fiber with the applied field due to the torque the field exerts on the fiber dipole, (c) oscillation of the fiber by means of an a.c. electric field perpendicular to the d.c. alignment field, (d) illumination of the fiber at normal incidence to its axis, and (e) detection of the light-scattering pulses from the oscillating fiber, in the direction of perpendicular to both the d.c. electric field and the direction of illumination. This approach differs somewhat from the continuous and complete (360^{o}) rotation used on the original FAM prototype.[11,12] In the new version the fiber axis oscillates about 26^{o} on either size of its midposition which coincides with the maximum of the detected light scattering pulse.

The electric field geometry and the scattering detection configuration of this new version† are shown in Figure 8. The d.c. field component is on the order of 3,000 V/cm thus producing a resultant field oscillation of $\pm$ 26.6^{o}. For the present carbon fiber application, an even somewhat smaller angular swing may be preferable, since the fibers of interest are considerably longer than those for which the FAM-1 was originally intended (to clarify this concept see later discussion on signal detection and processing). The degree of fiber alignment with respect to the applied electric field (i.e., the combined a.c. and d.c. fields) is an important aspect to be considered in the design of an instrument based on LISMEFA. It is of interest to note that, for conducteve fibers, the degree of alignment is essentially independent of the fiber length or its length-to-diameter ratio. This property is illustrated by the graph of Figure 9 which is obtained from the following

*Electric polarization is the separation and alignment of free charges in the fiber under the influence of the applied field creating an electric dipole. This charge separation is virtually instantaneous for conductive materials.

†Henceforth the discussion will always refer to the second generation d.c.-a.c. oscillation approach which is used in the commercial FAM-1 instrument.

BEGIN LAST LINE OF TEXT
BOTTOM OF IMAGE AREA OUTSIDE DIMENSION FOR TABLES AND ILLUSTRATIONS
3/8"

EPA-287 (Cin.) (4-76)

BEGIN FIRST LINE OF TEXT HERE
TYPING GUIDE SHEET
CENTER OF PAGE
TOP OF IMAGE AREA
DROPPED HEAD; BEGIN SECTIONS HERE

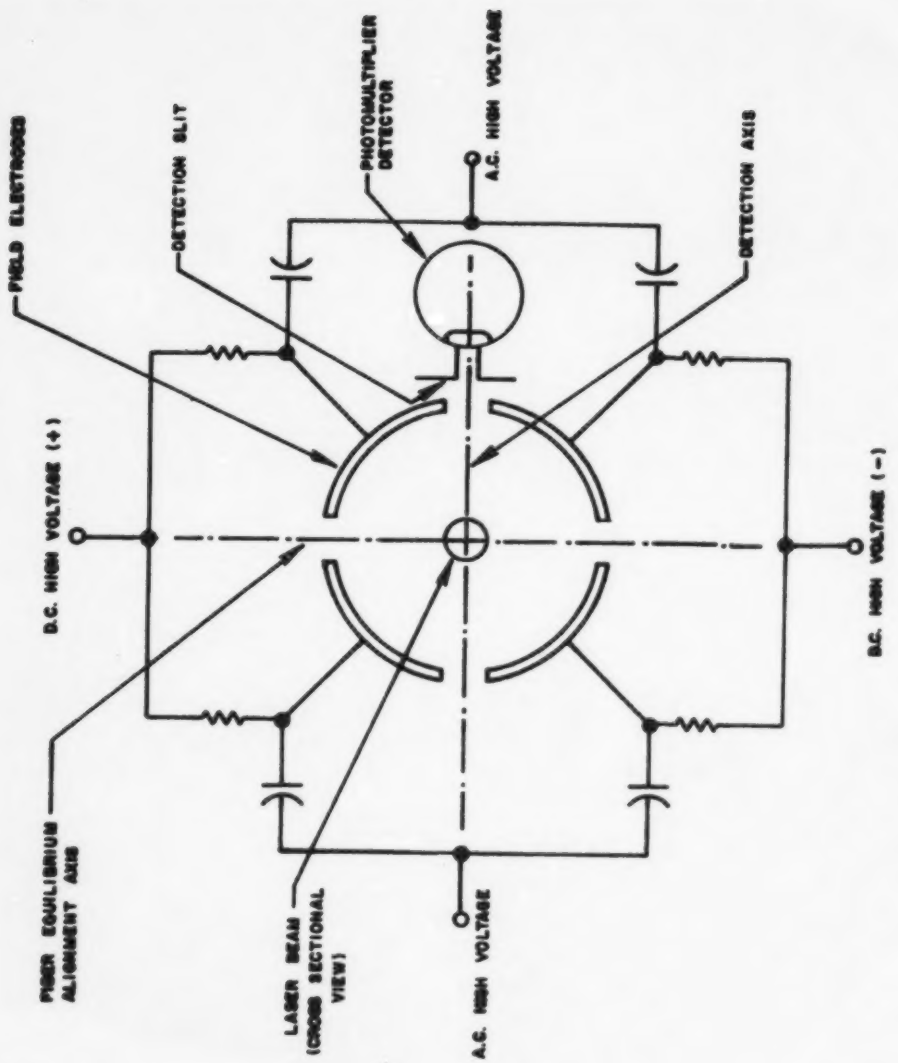

Figure 8. LISNEFA detection configuration.

BEGIN LAST LINE OF TEXT
BOTTOM OF IMAGE AREA; OUTSIDE DIMENSION FOR TABLES AND ILLUSTRATIONS
3/8"

EPA-297 (Cin.)
(4-76)

BEGIN FIRST LINE OF TEXT HERE
TYPING GUIDE SHEET
CENTER OF PAGE
TOP OF IMAGE AREA
DROPPED HEAD; BEGIN SECTIONS HERE

by the graph of Figure 9 which is obtained from the following relationship, whose derivation will not be repeated here.[11,12]

The degree of fiber alignment within the electric field can be defined by:

$$\theta' = 1/2 \arcsin \frac{48 \times 10^3 \mu \omega (\ln 2\beta - 1)}{E^2 (2 \ln 2\beta - 1)} \quad (6)$$

where, in m.k.s. units (SI):

θ' is the phase angle between the electric field vector and the fiber axis (radians)

ω is the angular oscillation rate (radian/sec)

E is the electric field intensity

For a field intensity of 3,000 V/cm, as shown in Figure 9, the phase lag between the conductive fiber axis and the applied oscillating field is less than 0.1° for the length-to-diameter ratios ranging from less than 10 to as much as 10,000 *i.e., corresponding to lengths of 50 μm to 50 mm).

Thus, in practice, essentially full fiber alignment and oscillation at frequencies of several hundred hertz is limited only by instrument dimensional considerations. The FAM-1 with a sensing duct inner diameter of about 12 mm can be applied to carbon fibers of up to about 1 or 2 mm in length. Longer carbon fibers would result in excessive field distortion and the possibility of sparkover within the LISMEFA sensing region. This is the principal reason for which a scaled-up and modified version of the FAM-1 sensing system would be required for the sensing of airborne carbon-graphite fibers whose length can reach 10 or 20 mm.

Light Scattering Signal

For the optical configuration considered here, the axis of the scattering fiber rotates in a plane normal to the direction of the illuminating beam; i.e., the case of perpendicular incidence of light on the fiber axis which is equivalent to a constant and maximum illuminating beam and the particle-detector axis, is about 90° in this case. For this angle the modulation of the detected scattered light is a maximum; i.e., the intensity variations are largest as the fiber is made to oscillate.[11]

Scattering under these conditions exhibits a very sharp maximum when the fiber is viewed perpendicularly; the scattered light is similarly concentrated in a tight beam as in the case of a search-light. The sharpness of this scattering pattern; i.e., the detected light pulse narrowness, is determined by the length of the fiber.

The angular light scattering function for cylinders is approximately[11,12,13]

$$I = I_o \frac{L^2}{\pi^2 r^2} \left(\frac{\sin \pi L \theta\lambda}{\pi L \theta/\lambda} \right)^2 T^2(\phi) \quad (7)$$

BEGIN LAST LINE OF TEXT
BOTTOM OF IMAGE AREA; OUTSIDE DIMENSION FOR TABLES AND ILLUSTRATIONS
3/8"

PAGE NUMBER
EPA-287 (Cin.)
(4-76)

BEGIN FIRST LINE OF TEXT HERE
TYPING GUIDE SHEET
CENTER OF PAGE
TOP OF IMAGE AREA
DROPPED HEAD: BEGIN SECTIONS HERE

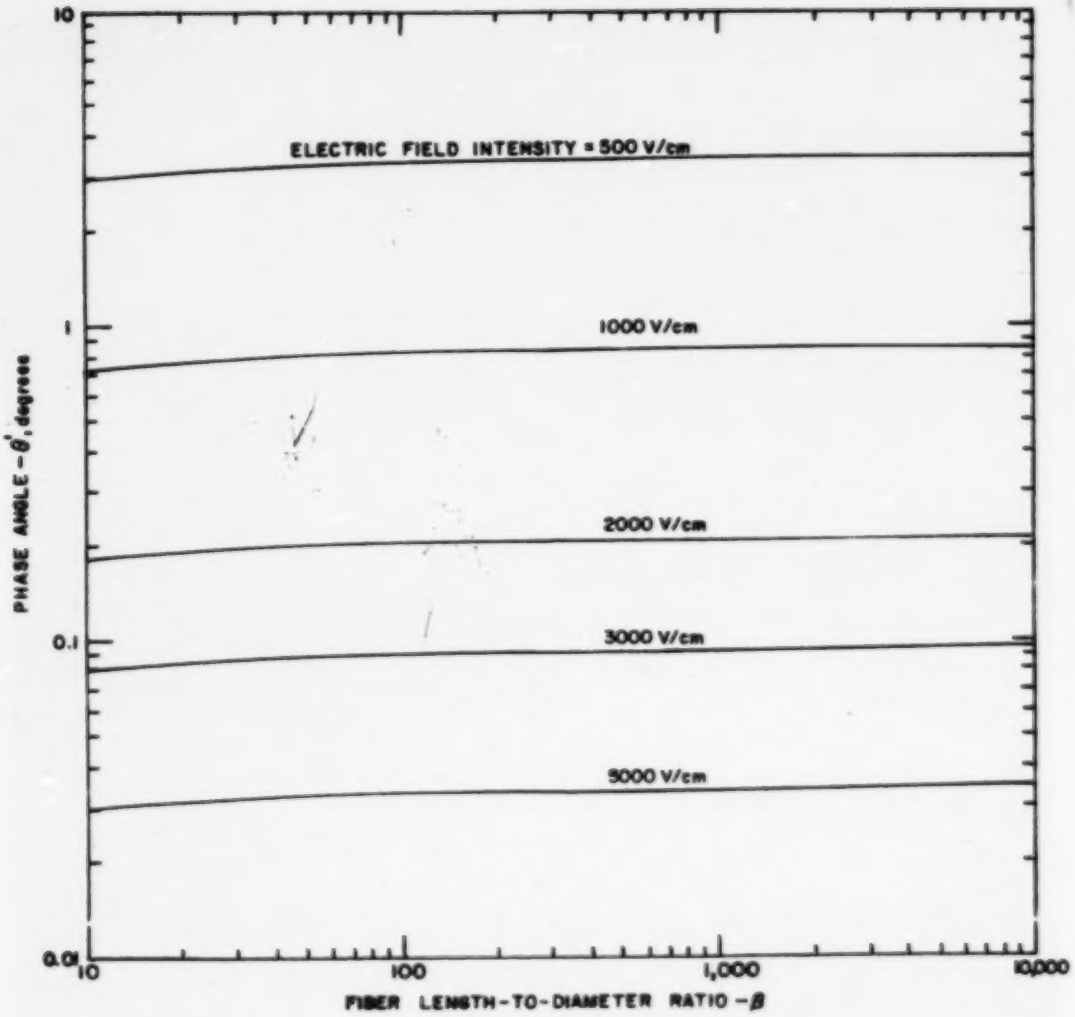

Figure 9. Degree of conductive fiber orientation for an oscillation electric field at 400 Hz, whose configuration follows that of Figure 8.

BEGIN LAST LINE OF TEXT
3/8"
BOTTOM OF IMAGE AREA. OUTSIDE DIMENSION FOR TABLES AND ILLUSTRATIONS

PAGE NUMBER
EPA-287 (Cin.)
(4-76)

BEGIN FIRST LINE OF TEXT HERE
TYPING GUIDE SHEET
CENTER OF PAGE
TOP OF IMAGE AREA
DROPPED HEAD; BEGIN SECTIONS HERE

where, L is the fiber length

λ is wavelength of the illuminating light beam

θ is the fiber axis angle in the plane of rotation

(θ = 0 defined as broadside viewing of the fiber)

ϕ is the scattering angle (about 90^{o} for this case)

r is the distance between the fiber and the detector

T (ϕ) is a complicated function of ϕ, λ, the fiber diameter and its index of refraction; T (ϕ) is a constant, however, for a given optical configuration and for a given particle composition (carbon in this case).

As a given fiber passes through the LISMEFA detection region, its oscillation is detected as a series of light pulses precisely separated in time. For the FAM-1 about 40 such pulses are observed for each fiber. An example of such a typical pulse train resulting from the passage of a single graphite fiber is depicted in Figure 10. This oscillograph shows the characteristically sharp scattering pulses resulting from a fiber whose length is estimated to be of the order of 50 to 100 μm. Figure 10 actually demonstrates the ability of the FAM-1 to detect carbon fibers which were aerosolized, from a ground-up mat provided by Union Carbide, by means of a small fluidized-bed generator developed at GCA, based on a similar design described by Spurny et al.[24]

As discussed in the background literature,[11,12] the LISMEFA technique requires the use of a collimated, monochromatic polarized light source. Helium-neon gas lasers fulfill these criteria and probably would be used for the present application. In order to minimize fiber detection coincidence errors, i.e., those resulting from the concomitant presence of more than a single fiber within the detection region, and in order to maximize the signal-to-noise ratio, the laser beam diameter must be kept at a minimum in the detection region. For reasons of design simplicity it has been found preferable to use the beam directly as generated by the laser, withoug either beam expansion or contraction. The general configuration of the optical-flow system of the FAM-1 is shown in Figure 11. With typical beam and LISMEFA sensor dimensions, maximum fiber concentrations of about 30 to 50 cm^{-3} can be accepted with reasonably low coincidence errors, without stream dilution.

Typical He-Ne laser beam diameters are of the order of 0.5 to 1 mm and thus some of the larger fibers would only be partially illuminated by the beam, after being aligned by the electric field. This would preclude the determination of fiber length for those longer than the beam diameter. However, information on the minimum fiber length is still available in this case; i.e., the fiber length can still be specified as being longer than y, the beam diameter. Shorter lengths than y can be measured by the pulse sharpness method.

The fiber length determination in the FAM-1 is obtained from the scattering signal pulse sharpness; i.e, longer fibers exhibit sharper, narrower

BEGIN LAST LINE OF TEXT
BOTTOM OF IMAGE AREA
INSIDE TENSION TABLES AND ILLUSTRATIONS
3/8"

EPA-287 (Cin.)
(4-76)

BEGIN FIRST LINE OF TEXT HERE
TYPING GUIDE SHEET
CENTER OF PAGE
TOP OF IMAGE AREA
DROPPED HEAD: BEGIN SECTIONS HERE

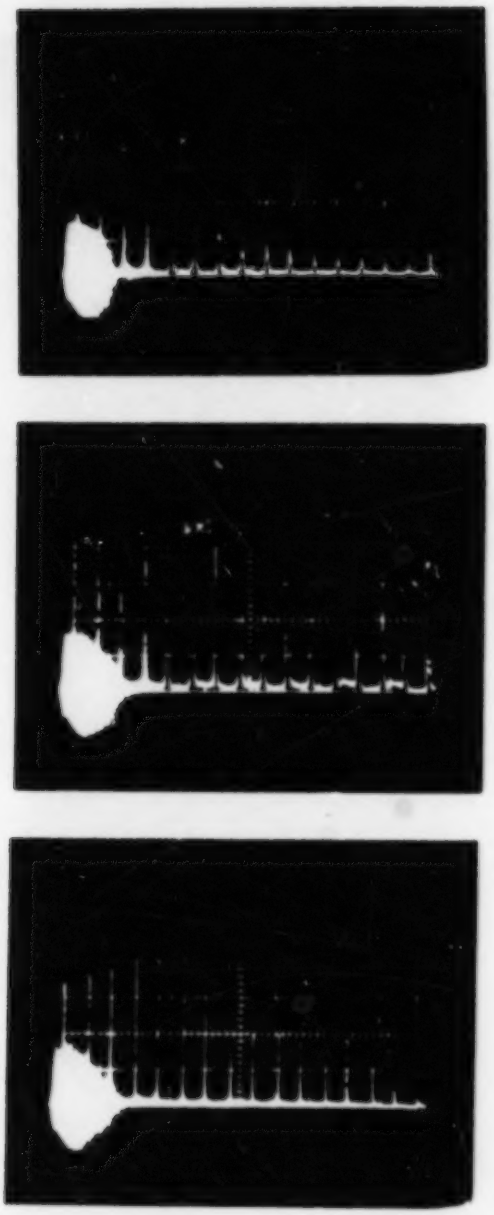

Figure 10. Typical FAM-1 Carbon Fiber Pulse Trains (1.25 msec pulse separation).

BEGIN LAST LINE OF TEXT
BOTTOM OF IMAGE AREA OUTSIDE DIMENSION FOR TABLES AND ILLUSTRATIONS
3/8"

EPA-287 (Cin.)
(4-76)

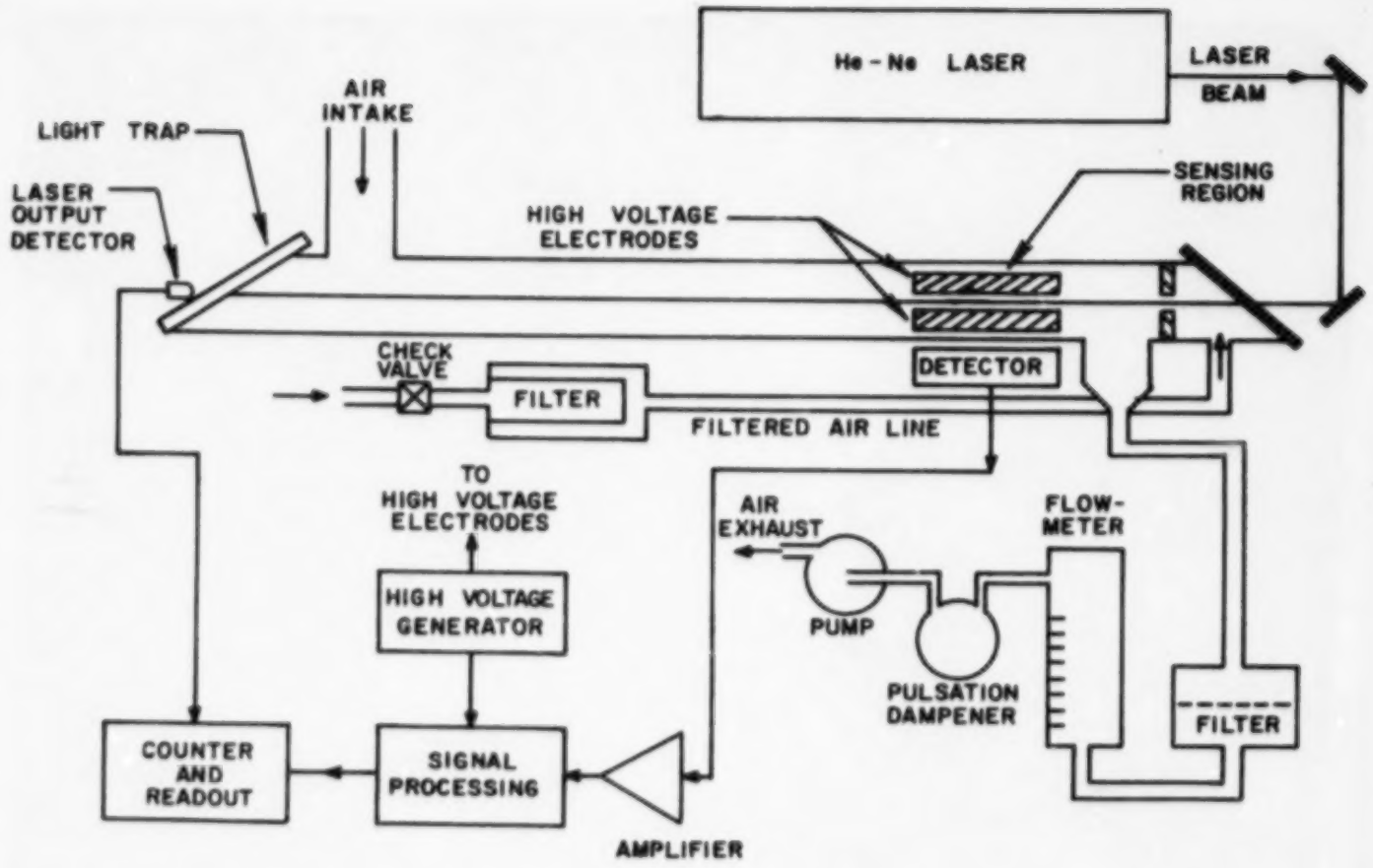

Figure 11. FAM-1 optics-flow diagram.

pulses. This behavior can be inferred from inspection of Equation (7): the factor $(\frac{1}{x} \sin x)^2$, where $x = \pi L \theta/\lambda$, becomes narrower as L increases.

The value of L can thus be obtained from the ratio of pulse amplitude to pulse average (or area). This ratio, whose derivation is in the literature,[11] is related to fiber length as:

$$L = \frac{\lambda}{4\pi} \frac{I \text{ peak}}{I \text{ average}} \quad (8)$$

Once the fiber length has been determined, and if the particle index of refraction is known as in the present case, the fiber diameter can be obtained from either peak or the average signal amplitudes.

LISMEFA Signal Processing

A summarized description of the electronic signal processing approach used on the FAM-1 will be presented here.

The purpose of this circuitry is to provide a high degree of detection selectivity for fibrous-shaped particles and to provide fiber length information.*

The LISMEFA electronics description will be in reference to the overall block diagram of Figure 12.

The light scattering pulses are detected by a photomultiplier tube and subsequently amplified, d.c.-blocked (to remove any steady-state bias components), and inverted to provide both an uninverted and an inverted signal to be processed by the lock-in or synchronous amplifier.

The oscillator provides the timing pulses for gating the input signal pulses into the 16 channels of the signal eductor, which operates in either of two modes: the integrating mode, or the output mode. The "flip-flops," arranged as a binary counter, select the proper signal eductor channel. Once the 16 channels pass through the integration process, the "analog-integrate" switch is opened. This results in the peak output of the central eight eductor channels to be sampled by the "peak" amplifier.

The signal average value of the 16 integrator channels is obtained by summing the levels of each channel to the summing amplifier. The signal average is voltage-divided by means of a panel adjustable "ratio" control potentiometer, and then compared with the signal peak, by means of an electronic comparator. If the peak exceeds the selected average, and if this peak exceeds the setting of a "threshold" control, then the logical "and" criteria are met and the results are clocked into a shift register. The comparison is performed for each of the eight central eductor channels, thus resulting in eight shift register pulses per cycle. The shift register is 128 bits long and there are outputs every 16 bits. These outputs are summed

*The original design objectives of the FAM-1 required only fiber length determination.

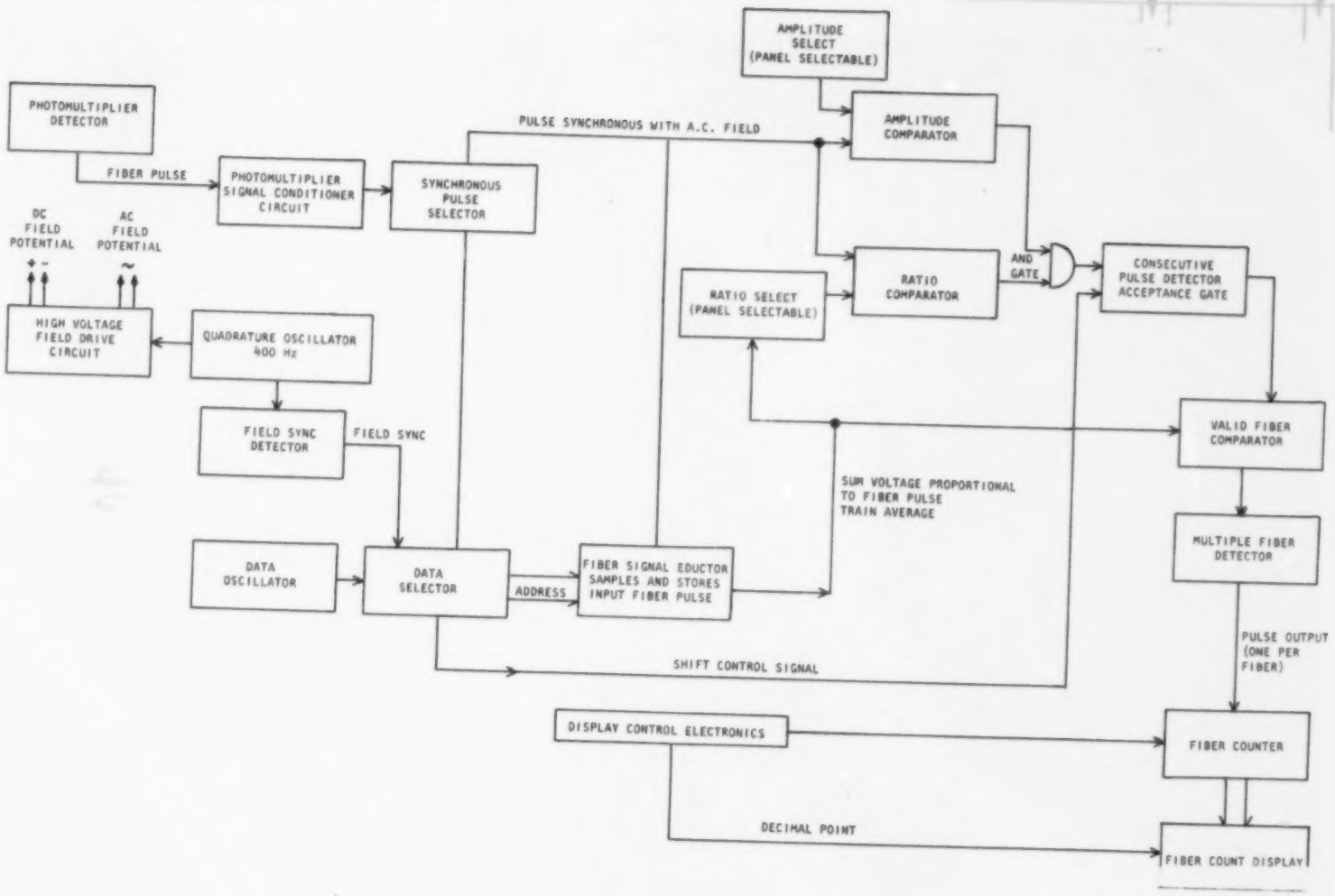

Figure 12. FAM-1 overall block diagram.

to a comparator so that at least 6 out of 8 inputs must be high to exceed a predetermined level in order to trigger a "one-shot," which when triggered remains on for 20 msec to bring the level of the 20 msec integrator up to trigger the final count pulse comparator. This implements the criteria that at least one channel of the signal eductor must have its peak greater than a certain threshold, as well as a certain ratio of the average signal, for 20 msec, in order for a signal to be accepted and counted as a fiber. The only additional criterion for acceptance is that the average signal be greater than zero for the same 20 msec. Once a fiber count pulse is received, the signal pulses are ignored for 50 msec to the signal board to reset itself and be in readiness for the next fiber signal pulse train.

The specific averaging, pulse sampling and dead times are, of course, adjustable and could be optimized for its application to carbon-fiber sensing depending on the requirements of maximum fiber concentration, flow rate, response time, etc.

The basic fiber alignment and oscillation field drive is obtained from a 400 Hz oscillator which has both sine and cosine outputs (i.e., 90° phase shifted). By adding these two a fixed 45° phase shift is obtained to drive the high voltage transformer primary, whose secondary is connected through capacitive coupling to the deflection electrodes as shown in Figure 8. The 400 Hz sine and cosine signals are also used to provide the reference pulses for the synchronous detection and gating functions described above.

The high voltage transformer output, in addition to providing the a.c. oscillation field, also serves to generate the steady-state d.c. fiber alignment field, by means of rectification and filtering of the 400 Hz high voltage.

AIRBORNE CARBON FIBER IN-SITU MONITORING BY PHOTO-THERMAL DETECTION

Introduction

One of the objectives of the present program was to select a monitoring technique capable of providing a means for the specific detection, characterization and measurement of airborne carbon fibers. This technique must be capable of determining the fibrous shape of these particles, as well as their predominantly carbonaceous composition, in the presence of interfering aerosols of various particle sizes, shapes and composition. Ideally, the presence of each sampled carbon fiber should be detected and counted, and these fibers should be sized (both their diameter and length), and their mass determined.

The *a priori* conclusion may be reached that no single technique can provide a complete solution to this problem. A combination of judiciously selected methods, however, appears extremely promising, and will be summarized in this section.

Initially, such a hybrid technique for the measurement of carbon fibers was considered by GCA. It relied on the implementation of two consecutive or sequential detection schemes whose principles and operation are independent of each other: a fiber shape characterization stage (FAM

BEGIN FIRST LINE OF TEXT HERE
TYPING GUIDE SHEET
CENTER OF PAGE
TOP OF IMAGE AREA
DROPPED HEAD, BEGIN SECTIONS HERE

technique), followed by a spark discharge configuration to identify its composition. This overall approach, although feasible in principle, relied on time-delayed sequential coincidence detection of a given fiber, and its destructive collection at the spark gap stage, both potential disadvantages affecting the reliability of a monitoring system incorporating this technique.

A method for the complete in-situ characterization with concurrent fiber shape and carbon detection, as well as fiber sizing and mass determination within a single sensing stage will now be described, including a theoretical analysis and a preliminary calculation of its essential design parameters.

One of the unique properties of carbon particles, and thus of fibers of this material, is the high degree of optical absorption they exhibit in the visible part of the electromagnetic spectrum.[25] Most noncarbonaceous airborne particles encountered in typical emission and ambient situations are of dielectric nature and are thus essentially pure light scatterers. Carbon particles have a complex index of refraction; i.e., with a substantial imaginary component whose magnitude is related to their absorptive properties. Typical values of this complex index of refraction for the carbon fibers range from 1.8 to 2.7 for the real part, and 0.7 to 1.6 for the imaginary one, for visible light. In comparison, materials such as quartz have an index of refraction whose real part is 1.544 with a negligible imaginary part (i.e., less than 10^{-6}). This light-absorptive property of carbon has been applied for its detection in collected samples of aerosol particles by means of photoacoustic analysis.[26]

Recent years have seen a rapid development of photoacoustic spectroscopy (PAS) as a powerful technique for trace gas and solids analysis. PAS is based on the absorption of radiation (U.V., visible and/or IR) by a sample (gaseous or solid) contained within a closed gas-filled cell whose pressure increases as a result of the radiation-induced increase in temperature of the sample. By modulating the radiation, the corresponding pressure modulation can be sensed by a microphone in the interior of the cell. As mentioned above, a recent application of this technique has been the detection of carbon contained in urban aerosol samples by irradiating it with an intensity modulated He-Ne laser beam.[26]

A distinct variation of this technique is the direct, in situ, sensing of the black-body (or gray-body) infrared emission of carbon fibers irradiated by a beam of light. Whereas nonabsorbing particles will behave essentially as thermal emitters at the stream temperature, carbon particles or fibers, however, as a result of their increased temperature exhibit significantly enhanced thermal emission, shifted to shorter wavelengths. This fiber irradiation-thermal detection can be performed within a modified LISMEFA (Light Scattering Modulation by Electric Field Fiber Alignment and Rotation) stage. The laser beam would be used not only to generate the light scattering signal pulses characteristic of fibers, but would also serve to raise the fiber temperature (if it is composed of carbon). An infrared detector (in addition to the usual optical scattering detector) will sense the enhanced wavelength-shifted thermal emission from the optically absorbing fibers. The infrared signal will also exhibit a modulation of the same frequency as that

BEGIN LAST LINE OF TEXT HERE
BOTTOM OF IMAGE AREA OUTSIDE DIMENSION FOR TABLES AND ILLUSTRATIONS
3/8"

PAGE NUMBER
EPA-257 (Cin.) (4-76)

BEGIN FIRST LINE OF TEXT HERE
TYPING GUIDE SHEET
CENTER OF PAGE
TOP OF IMAGE AREA
DROPPED HEAD, BEGIN SECTIONS HERE

of the scattering pulses; i.e., synchronous with the electric-field-induced fiber oscillation or rotation thus permitting high-selectivity noise filtering by means of synchronous phase-sensitive signal processing. Wave shape of the infrared signal would, however, be uniquely different from the light scattering pulse train associated with the passage of each fiber. The information contained within the two signals, scattering and thermal emission, would be sufficient to fully characterize a detected particle as a fiber composed of carbon through a coincidence criterion. Fiber length, diameter and mass can also be derived by means of an algorithm applied to the analysis of the two signals.

One problem that may affect the above described thermal detection method is the potential variability of the temperature of the effluent stream to be sampled. Elevated gas temperatures would result in high thermal noise levels and the decreased ability to distinguish carbon fibers from those of differing composition. Controlled temperature air dilution may then be required to control the thermal background conditions and thus provide a sufficient temperature (and corresponding wavelength) separation with respect to the thermal emission and signal of interest. In addition, modulation (i.e., chopping) of the laser beam in synchronism with the electric field oscillation may provide additional signal-to-noise enhancement. Ideally, the higher the temperature to which the fiber can be raised, the larger the resulting infrared emission, and a corresponding enhancement of the signal-to-noise ratio at the IR detector. Practical limits, however, are given by the required laser power and the ignition temperature of the carbon fiber in air, which is typically between 750°K and 900°K, depending on the type of carbon fiber (i.e., graphite versus amorphous carbon).

Fiber length is determined from the pulse shape of the light scattering signal, whereas fiber projected area will be obtained from the infrared signal. Fiber mass can then by derived from its dimensions and its composition (i.e., carbon). Fibrous shape is determined principally by the light scattering signal, but would be confirmed by the thermal detection signature. Carbon composition would be uniquely obtained from the thermal signal. A noncarbonaceous fiber would be detected as a fiber by light scattering, but would not be sensed by the IR detector.

Determination of Design Parameters

The method of photo-thermal detection (henceforth PTD) described above is based on the temperature rise that carbonaceous particles undergo when irradiated by a light beam (e.g., from a laser). The resulting thermal emission can be distinguished from that of other particles because of the significantly higher temperature that absorbing (i.e., carbon) particles achieve.

In order to establish the theoretical feasibility of this method, several parameters must be determined: (a) the required laser power, (b) the time constant of the particle temperature rise, (c) the detected signal intensity, and (d) the signal-to-noise ratio.

BEGIN LAST LINE OF TEXT
BOTTOM OF IMAGE AREA, OUTSIDE DIMENSION FOR TABLES AND ILLUSTRATIONS

EPA-287 (Cont.) (4-76)

Temperature Rise and Thermal Time Constant--

The temperature, T_s, to which a spherical particle rises can be obtained from:[27]

$$T_s = T_o + P_L Q_{abs} a/4k_a(1-e^{-t/\tau_s}) \quad (9)$$

where τ_s is the thermal time constant = $a^2\rho_p C_p/3k_a$

T_o is ambient absolute temperature

P_L is power density of the irradiating beam on the particle

k_a is the thermal conductivity of the air

t is the time

a is particle radius

C_p is specific heat of the particle

ρ_p is particle density

Equations (9) and (10) are specific solutions of the partial differential heat conduction equations, for the spherically symmetric case. No such solution has been evolved for acicular-shaped particles, however, a first order approximation, based on the assumption of a cylinder of total area equal to that of a sphere of radius a, yields a temperature T_c:

$$T_c = T_o + P_L Q_{abs} \left(\frac{rl}{2}\right)^{\frac{1}{2}} \frac{1}{4ka} (1-e^{-t/\tau_c}) \quad (11)$$

$$\tau_c = \frac{rl\rho_p C_p}{6ka} \quad (12)$$

and*

where r is the cylinder radius
l is the cylinder length

Signal Detection Parameters--

The total power density at the detector due to the thermal emission from a heated carbon fiber is given by:

$$P_d = \frac{A\sigma\varepsilon T_c^4}{4\pi R^2} \quad (13)$$

where P_d is the total power/area at the detector; i.e., over all wavelengths

A is the fiber total area

σ is the Stefan-Boltzman constant = 5.67×10^{-12} W cm^{-2} $^oK^{-4}$

ε is fiber emissivity in the infrared

*Equation (12) can also be obtained by a similar manipulation of the thermal time constant equation given by Terhune and Anderson.[28]

BEGIN FIRST LINE OF TEXT HERE
TYPING GUIDE SHEET
CENTER OF PAGE
TOP OF IMAGE AREA
DROPPED HEAD; BEGIN SECTIONS HERE

T_c is the absolute temperature of the fiber

R is the distance between the fiber and the infrared detector.

The total (i.e., broadband) signal-to-noise ratio, S/N, assuming non-absorbing interfering particles of equal size as those of the carbon fibers of interest, can be calculated from:

$$S/N = \left(\frac{T_c}{T_o}\right)^4 \qquad (14)$$

By using a wavelength band-pass filter around the thermal emission peak wave length of the carbon fibers, a further drastic enhancement of the signal-to-noise ratio can be achieved. A typical wavelength filter will be included and its effect on S/N will be calculated in the subsequent presentation of a specific example.

The wavelength at which the maximum thermal emission occurs is given by Wien's displacement law:

$$\lambda_m = \frac{2897.9}{T} \qquad (15)$$

where T is the absolute temperature, in ^oK

λ_m is the wavelength of peak emission, in m

Figure 13 is a plot of black-body thermal emission for two temperatures, 300^{o}K (i.e., essentially ambient), and 700^{o}K, a temperature to which a carbon fiber sould be raised in air without concomitant combustion. From the curves of Figure 13 it is apparent that a temperature rise of 300^o to 700^{o}K results in a vastly enhanced thermal emission accompanied by a significant shift towards the shorter wavelengths, both effects contributing to separating the carbon fiber produced signal from the noise associated with all other non or weakly absorbing particles.

Example Design Calculation

A specific case will be calculated through in order to determine typical system parameters and to ascertain the practical feasibility of the approach.

The following case will be assumed:

- Carbon fiber with a diameter of 8 μm and a length of 100 μm.
- Ambient, or diluted, air temperature of 300°K.
- Final fiber temperature of 700°K.
- Residence time, t of equation (11), within laser beam of the order of 0.5 sec (corresponding to a residence time within the detection region of about 0.05 sec).

BEGIN LAST LINE OF TEXT
BOTTOM OF IMAGE AREA, OUTSIDE DIMENSION FOR TABLES AND ILLUSTRATIONS
3/8"

PAGE NUMBER
EPA-287 (Cin.)
(4-76)

BEGIN FIRST LINE OF TEXT HERE
TYPING GUIDE SHEET
CENTER OF PAGE
TOP OF IMAGE AREA
DROPPED HEAD: BEGIN SECTION HERE

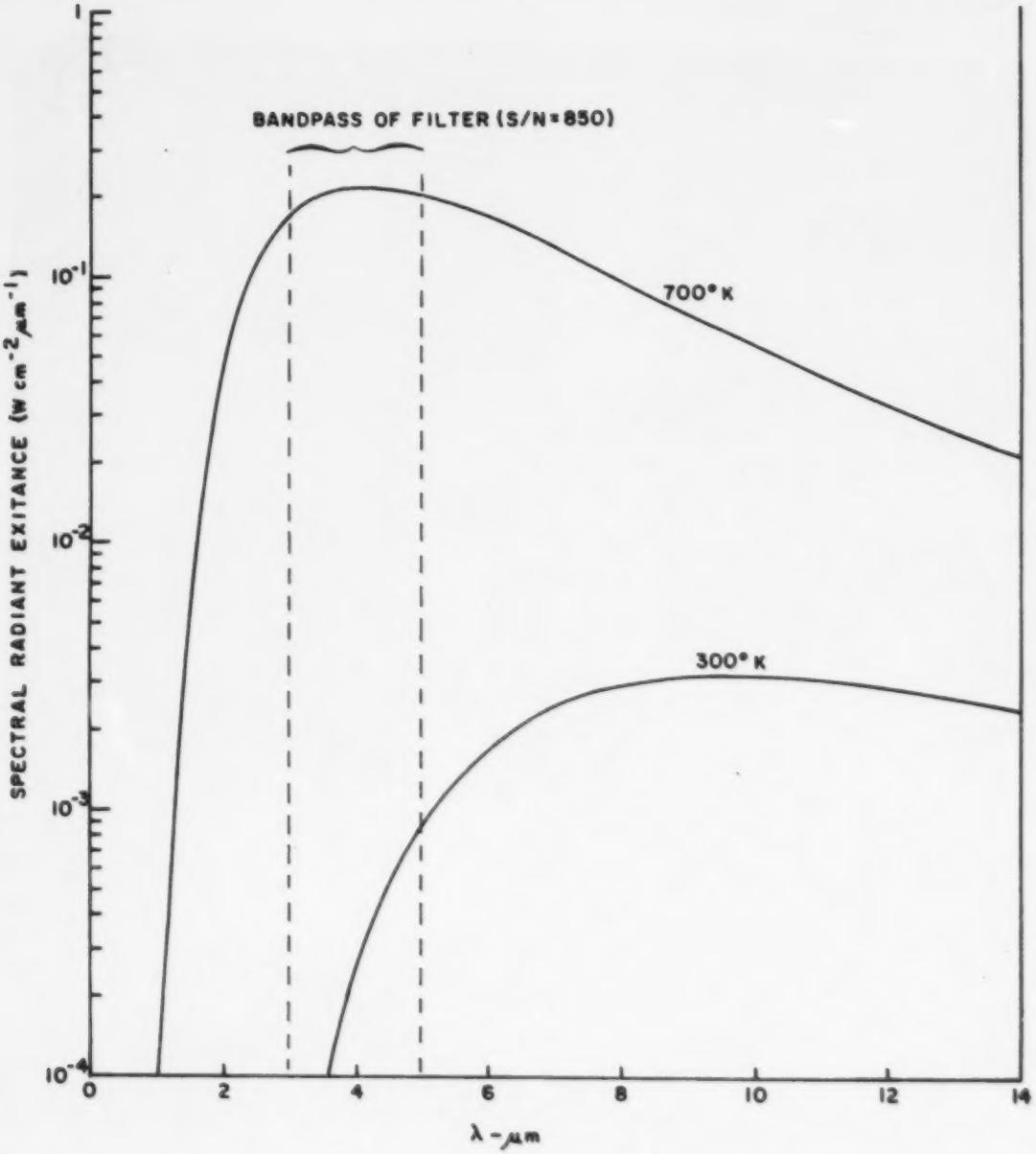

Figure 13. Black-body emission as a function of wavelength and absolute temperature. Bandpass of filter assumed in text is shown as dashed lines.

BEGIN LAST LINE OF TEXT
3/8"
BOTTOM OF IMAGE AREA. OUTSIDE DIMENSION FOR TABLES AND ILLUSTRATIONS

EPA-257 (Cin.)
(4-76)

BEGIN FIRST LINE OF TEXT HERE
TYPING GUIDE SHEET
CENTER OF PAGE
TOP OF IMAGE AREA
DROPPED HEAD: BEGIN SECTIONS HERE

- The absorption efficiency, Q_{abs} of Equation (10), for carbon particles is nearly unity for diameters exceeding about 0.2 μm at visible light wavelengths (e.g., assuming the use of a He-Ne laser to irradiate the carbon fibers).

- Other parameters of Equations (11) and (12) are:[29]

$$k_a = 2.59 \times 10^{-4} \text{ joule sec}^{-1} \text{ cm}^{-1} {}^{o}K^{-1}$$

$$\rho_p = 2.25 \text{ g cm}^{-3}$$

$$C_p = 0.711 \text{ joule g}^{-1} {}^{o}K^{-1}$$

Replacing the above values in Equations (11) and (12) we obtain:

$$\tau_c = 4.1 \times 10^{-3} \text{ sec} = 4.1 \text{ msec}$$

thus, the factor $(1-e^{-t/\tau_c})$ of Equation (11) is essentially unity for a residence time t = 500 msec; i.e., thermal equilibrium is exhibited between the radiation impinging on the carbon fiber and its infrared emission. Therefore, from Equation (11) we obtain:

$$P_L = 290 \text{ watts cm}^{-2}$$

Assuming a 1 mm diameter laser beam, this power density corresponds to a laser beam power, P_L, of:

$$P_L = 2.3 \text{ watts}$$

This amount of power is certainly not obtainable directly from standard He-Ne lasers, and would require an exceedingly expensive and cumbersome Ar, Kr, CO_2, etc., laser. Fortunately, the above power density can be achieved by means of intracavity illumination within a small (2 to 5 mW) He-Ne laser. This approach was developed by Knollenberg[30] and incorporated in commercially-available instrumentation. This method consists of replacing one of the mirrors of the laser column by a transparent window and placing the mirror such that the air stream to be monitored becomes part of the resonant laser cavity.[31] As a result, the illumination intensity to which the particles are exposed is increased by typical factors of 500 to 600 with respect to the radiation emerging from the standard type of He-Ne laser.[30] Thus, a laser rated at a standard 5 mW output can provide an intracavity illumination of the order of 2.5 to 3W, which would be adequate for the present requirements based on the above calculation.

Assuming that:

$\varepsilon = 0.53$ in the IR (i.e., the minimum or worst-case value)[31]

R = 1 cm

BEGIN LAST LINE OF TEXT
BOTTOM OF IMAGE AREA; OUTSIDE DIMENSION FOR TABLES AND ILLUSTRATIONS
3/8"

PAGE NUMBER
EPA-287 (Cin.) (4-76)

BEGIN FIRST LINE OF TEXT HERE
TYPING GUIDE SHEET
CENTER OF PAGE
TOP OF IMAGE AREA
DROPPED HEAD; BEGIN SECTIONS HERE

we obtain replacing in Equation (13):

$$P_d = 1.44 \times 10^{-6} \text{ watts cm}^{-2}$$

Particles with negligible absorption; i.e., noncarbonaceous ones, will remain essentially at ambient stream temperatures (i.e., only scattering but not absorbing the laser illumination), and their total power density at the IR detector (assuming a nonabsorbing fiber of equal dimensions to that of the preceding example) would be only about $(300/700)^4 \times 1.44 \times 10^{-6} W/cm^2$ or 4.86×10^{-8} W/cm^2. In addition, by using a band-pass filter in the infrared, a drastic improvement of signal-to-noise-ratio can be achieved. For example, for a filter passing only 3.5 to 4.5 μm radiation (as can be seen from Figure 13, the peak of the thermal emission for 700 ± K is about 4.1 μm), the signal-to-noise ratio, for the above example would be of the order of 850.

A description of a practical sensing configuration incorporating the PTD technique will now be presented.

Preliminary Detection Configuration

Based on the above analysis a preliminary configuration for a carbon-fiber detection system will now be described.

One of the unique advantages of the photo-thermal detection technique is that it presents the possibility of combining it with the light scattering fiber identification method within one common sensing geometry. The laser beam required to raise the fiber temperature serves, at the same time, as the source of optical illumination required to produce the light scattering signature to characterize a particle as being a fiber.

Thus, the detection of thermal emission; i.e., the carbonaceous characterization, can be directly combined with the scattering detection; i.e., the fiber characterization, within a common sensing region.

A preliminary and simplified conceptual configuration incorporating the above mentioned system is depicted in Figure 14. The active laser cavity geometry mentioned previously is also shown in Figure 14. The optical and the thermal detectors are placed on opposite sides of the flow-detection duct, thus sensing their respective signals simultaneously as a fiber passes through the quadrupole field section that produces the alignment and oscillation of the fibers. Whereas the fiber-produced optical scattering pulses are sharply peaked (idiosyncratic of scattering by long cylinders), the thermal emission will exhibit a smooth oscillation resulting from the oscillation of the fibers which, in turn, result in a varying projected area as seen by the thermal detector. The scattering pulses and thermal fluctuations, however, will be synchronous and in phase because the scattering maxima occur when the fiber is perpendicular to the axis of detection, when the thermal sensor views the fiber at its maximum projected length.

The two detected signals contain a wealth of combined information which, using a proper signal processing algorithm, will provide a full characterization

BEGIN LAST LINE OF TEXT HERE
BOTTOM OF IMAGE AREA
INSIDE DIMENSION FOR TABLES AND ILLUSTRATIONS
3/8"

EPA-287 (Cin.)
(4-76)

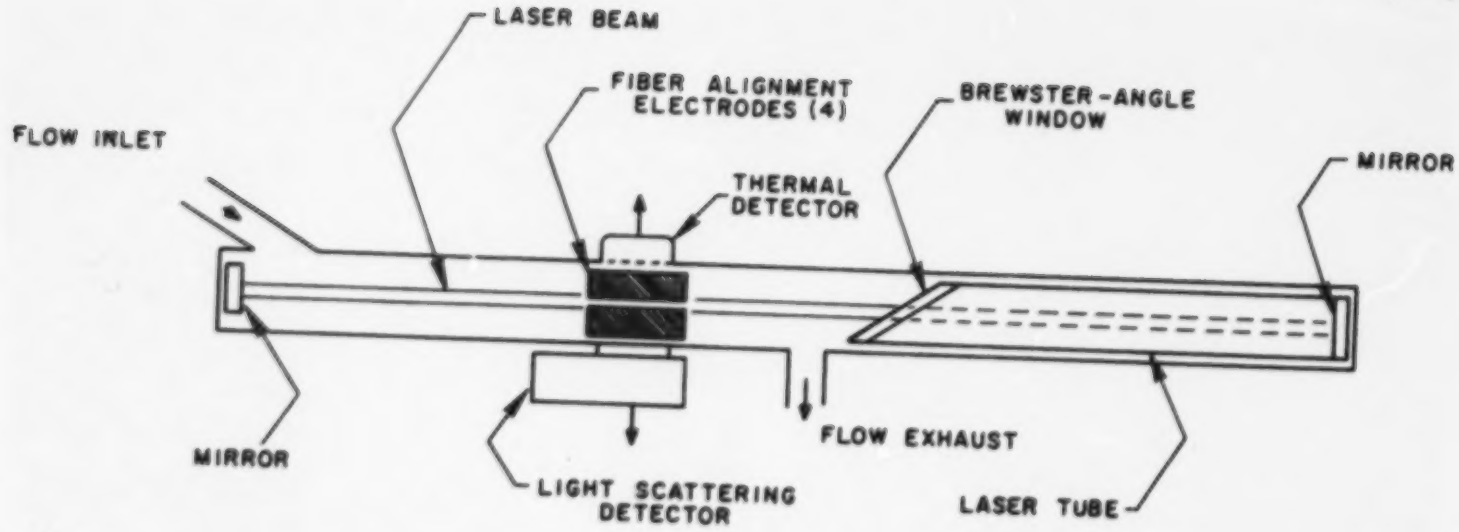

Figure 14. Simplified conceptual sensing system diagram of light-scattering-photothermal carbon fiber monitor.

Fiber composition (i.e., carbon or noncarbon), carbon fiber length, diameter and, by computation from the preceding parameters, carbon fiber mass can all be determined concurrently by the combined analysis of the two signals. Mutual confirmation; i.e., by coincidence detection signal processing of the outputs of the two detectors, will provide a greatly enhanced selectivity against spurious detection counts; i.e., only if both signals are present at the same time, and fulfill certain amplitude, shape and phase conditions, is the event accepted as a positive carbon fiber count. This concept is pictorially represented on Figure 15 which shows the basic decision-making steps to which the signal is subjected before it is accepted as being produced by a carbon fiber.

Scattering signal pulse height and area provide fiber length information, the fiber diameter is inferred from both the scattering pulse amplitude as well as the thermal signal amplitude, and mass is derived from length, diameter and the compositional informational; i.e., carbon, whose specific gravity is defined within practical limits of accuracy. As described previously, the peak of the thermal emission for a fiber temperature of 700°K (427°C) would be at an infrared wavelength of about 4 μm. There are several different types of detectors available in that general range. Thermopile, Hg Cd Te, lead-sulphide, lead-selenide, etc., detectors are now commercially obtainable, some with an integrated thermoelectric cooling element within a single miniaturized package, no larger than a transistor metal envelope. Some of these detectors can be obtained with an integral wavelength-selective window, such as the one mentioned before, with a band-pass of 3 to 5 μm.

In conclusion, the method of photo-thermal detection as applied to the sensing and characterization of airborne carbon fibers is based on imparting a significant temperature rise to the particles to be monitored, and sensing the thermal emission accompanying that temperature rise. Only highly optically absorbing particles; i.e., carbon particles, will exhibit this behavior, thus differentiating themselves from most other non- or weakly absorbing ones. Fiber shape characterization can be performed concurrently by the electric field-induced alignment and light-scattering method developed by GCA and implemented in the FAM instrument.

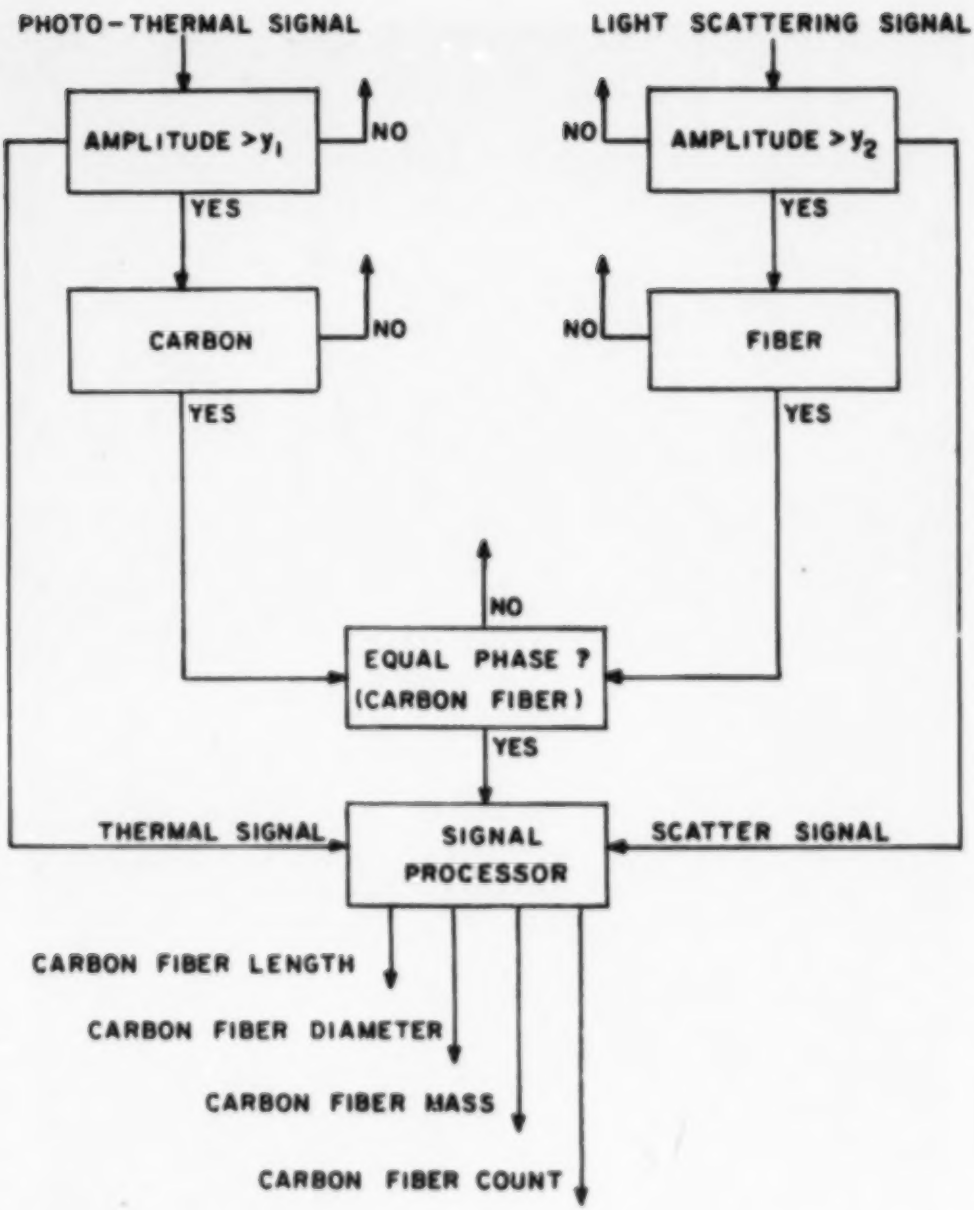

Figure 15. Conceptual signal flow chart of a photo-thermal-light-scattering carbon fiber monitoring system.

TYPING GUIDE SHEET
BEGIN FIRST LINE OF TEXT HERE
CENTER OF PAGE
TOP OF IMAGE AREA
DROPPED HEAD: BEGIN SECTIONS HERE

SECTION 6

APPLICABILITY AND COST ANALYSIS OF CANDIDATE METHODS

The contents of the preceding section of this report demonstrate the wide variety and range of potentially applicable methods of carbon fiber detection and assessment. Very few methods, if any, however, are available at present for the unequivocal identification and sizing of such airborne particles, and even less so, for their automated monitoring. Most of the techniques used heretofore are either cumbersome, or nonspecific to carbon fibers, or both.

Table 3 is a comprehensive summary of the state-of-the-art in carbon-graphite-fiber detection and measurement technology. Each of the methods discussed in Section 3 of this document is listed in Table 3. The detection specificity of each of these techniques is graded by its ability to discriminate carbon particles from those of predominantly noncarbon composition, by its specificity to fibrous shaped aerosols, and its combined selectivity to fibers composed mainly by carbon. The next column of Table 3 grades each method by its compatibility with automated, continuous or continual monitoring, i.e., without requiring intensive human intervention. Those methods that are potentially more compatible with source monitoring applications are so marked.

After a careful assessment of the methods discussed previously, it was concluded that a detailed cost analysis of each of these techniques and their multiplicity of possible variations would fall beyond the constraints of this project. Furthermore, two clearly different cost categories must be considered in this content: (a) the cost of development of a given technique in order to make it applicable to the specific requirement of continuous or continual source monitoring of carbon fibers, and (b) the eventual commercial sales price of a practical instrument based on the preceding developmental stage. Precise predictions of the latter cost are almost impossible, especially for those numerous cases where the developmental stage is incipient, partial or nonexistent at present.

It was thereforee decided that a qualitative categorization of costs would be more meaningful, both for the development effort as well as for the eventual commercial price. For the development category, the three categories have the following approximate equivalence:

(a) LOW--The technique has already been developed and tested. It may require a relatively small additional effort to finalize a practical design. This additional development cost would be on the order of $50,000 or less.

BEGIN LAST LINE OF TEXT HERE
BOTTOM OF IMAGE AREA OUTSIDE DIMENSION FOR TABLES AND ILLUSTRATIONS
PAGE NUMBER
EPA-287.1(Rev.) (4-76)

TABLE 3. SUMMARY TABULATION OF POTENTIALLY APPLICABLE TECHNIQUES TO THE DETECTION AND MEASUREMENT OF CARBON FIBERS, INCLUDING A QUALITATIVE COST ANALYSIS

Method	Detection specificity			Compatibility with autom. monit.	Cost		Observations
	Carbon	Fiber	Carbon-Fiber		Develop.	Commercial	
1. High Volt Spark	Med	Med	Med	High[a]	Low[a]	Med	Limited to fibers longer than 1 mm.
2. Brass Ball	Low	Med	Low	High[a]	Low[a]	Med	Limited to fibers longer than 2 mm.
3. Low Volt. Grid	Low	Med	Low	Med	Low[b]	Low	Unpredictable operation, low collection efficiency.
4. Cont. Optical Counter	Low	Low	Low	High[a]	Low[b]	Low	Nonspecific to C-fibers, insensitive.
5. Lidar	Low	Low	Low	High	Low[a]	High[d]	Nonspecific to C-fibers.
6. Microwave	Low	Med	Low	High	High[c]	High	
7. Sticky Tape	Low	High	Med	Low	Low[a]	Low[d]	Requires microscopy of collected sample.
8. Filter Screen	Low	High	Med	Low	Low[a]	Low[d]	Requires microscopy.
9. Spectrophone	High	Low	Low	Low[a]	Med[b]	High	See Photo-thermal detection as preferred technique.
10. Micro-Raman	High	Low	Low	Low	High[b]	High	
11. Optical Absorption	High	Low	Low	Med	Med[b]	Med	Requires collection of particles.
12. Angular Light Scat.	High	High	High	Low	Med[b]	High[d]	Limited usefulness except for LISMEFA (see No. 26).
13. Light Polarization	Low	High	Low	High	Med[c]	Med	Not useful for individual fiber detection.
14. Differential Conductivity	Low	Med	Low	Med	High[a]	Med[d]	Coulter-counting may be incompatible with conductive fibers.
15. Differential Elect. Mobility	Low	Med	Low	High[a]	Med[b]	Med	
16. Electr. Alignment	Low	High	Low	High[a]	Low[a]	Med[d]	This technique must be used in combination with other detection methods.
17. Magnetic Alignment	Med	High	Med	Med[a]	Med[b]	Med	Same as above.
18. Aerodyn. Alignment	Low	High	Low	High	Med[b]	Med	This technique must be used in combination with other detection methods.

(continued)

TABLE 3 (continued)

Method	Detection specificity			autom. monit.	Cost		Observations
	Carbon	Fiber	Carbon-Fiber		Develop.	Commercial	
19. Ultrasonic Effects	Low	Med	Low	High	High[c]	Med	Requires fiber alignment.
20. Video-Microscopy	Low	High	Med	Low	Med[a]	High[d]	Requires collection on a medium.
21. Spark Spectrometry	High	Low	Med	High[e]	Med[c]	Med	Requires other techniques for fiber identification.
22. Laser-Spark Spectrometry	High	Low	Low	High[e]	Med[b]	High	Same as above.
23. Scintillation Analysis	High	Low	Low	High	Med[b]	High[d]	Same as above.
24. X-Ray	High	Low	Low	Low	Med[a]	High[d]	Same as above.
25. Differential Light Scat.	High	Low	Low	High[e]	Med[c]	Med	Same as above.
26. LISMEFA	Low	High	Low	High[e]	Med[a]	Med[d]	Applied in GCA-FAM. Useful in combination with carbon-specific techniques.
27. Photo-thermal detection and Electric Alignment	High	High	High	High[e]	High[c]	Med	Highly specific to carbon fibers.

[a] Development largely completed.
[b] Partially developed
[c] To be developed.
[d] Commercially available.
[e] Potentially adaptable to source monitoring.

As applicable to the detection of carbon fibers.

(b) MED--The method has been researched, and applied to other or at best similar types of measurements. It requires additional efforts to evolve a practical system applicable to carbon fiber monitoring. Further development costs are on the order of $50,000 to $150,000.

(c) HIGH--This technique has not been explored sufficiently for this application, or its overall practicability has not been demonstrated empirically. A dedicated development effort is required whose cost equals or exceeds $150,000.

The present status of development of each of the candidate methods, as potentially applicable to the detection and measurement of carbon fiber is also indicated on this column.

The subsequent column categorizes the present, or future (i.e., estimated) commercial selling cost of instruments or devices based on each of the listed techniques. Present commercial availability of applicable or closely related instruments is also indicated.

The approximate commercial cost hierarchy is defined as follows:

(a) LOW--The cost of the presently available device or instrument or of an instrument eventually developed, is equal to or less than about $2,000.

(b) MED--Instrument cost, as defined in (a), between $2,000 and $10,000.

(c) HIGH--Instrument cost, as defined in (a), exceeding $10,000.

REFERENCES

1. National Aeronautics and Space Administration, Washington, D.C. A Report of Observed Effects on Electrical Systems of Airborne Carbon/Graphite Fibers. NASA Report No. TM78652, January 1978.

2. Wagman, J., H. R. Berger, J. L. Miller, and W. D. Conner. Dusts and Residues from Machining and Incinerating Graphite/Epoxy Composites. EPA-600/2-79-196, Nov. 1979.

3. Reynolds, W. N. Physical Properties of Graphite. Elsevier, London, 1968.

4. Fuchs, N. A. Mechanics of Aerosols. New York Paramon Press, 1964.

5. Friedlander, S. K. Smoke, Dust and Haze. John Wiley & Sons, 1977.

6. Crane, R. I., and R. L. Evans. Inertial Deposition of Particles in a Bent Pipe. J. Aerosol Sci., 8:161, 1977.

7. Yang, L. C. High Voltage Spark Carbon Fiber Detection System. JPL Publication 80-30, April 1980.

8. NASA Risk Analysis, NASA Conference Publication 2074. Carbon Fiber Risk Analysis. An Industry/Government briefing held at Langley Research Ctr., Hampton, Virginia, Oct. 31-Nov. 1, 1978, pp. 1-248.

9. Truex, T. J., and J. E. Anderson. Mass Monitoring of Carbonaceous Aerosols with a Spectrophone. In: Carbonaceous Particles in the Atmosphere, LBL, Univ. of California, March 1978.

10. Rosen, H., A. D. Hansen, L. Gandel, and T. Nova-Kov. Identification of the Graphitic Carbon Component of Source and Ambient Particulates by Raman Spectroscopy and an Optical Attenuation Technique. In: Carbonaceous Particles in the Atmosphere, LBL, Univ. of Calif., p. 49, March 1978.

11. Lilienfeld, P., and P. B. Elterman. Development and Fabrication of a Prototype Fibrous Aerosol Monitor (FAM). EPA-600/7-77-147, December 1977.

12. Lilienfeld, P., P. B. Elterman, and P. Baron. Development of a Prototype Fibrous Aerosol-Monitor. AIHA Journal, 40:270, 1979.

13. Detenbeck, R. W., and D. R. Hemenway. Development of a Two-Detector, Optical, Aerosol-Fiber Counter. Paper No. 246, AIH Conference, Chicago, May 1977.

14. Davies, R., R. Karuhn, J. Graf, and J. Stockham. The Rapid Counting and Sizing of Fibers in a Mixture Using an IITRI-modified Coulter-Counter. Am. Ind. Hygiene Assoc. J., 36:825. 1975.

15. Fedrick, N. A., A. T. Bell, and D. N. Hanson. Particle Counting by Glow Discharge Perturbation. Env. Sci. Tech., 6:117, 1972.

16. Zebel, A., D. Hochrainer, and C. Boose. A Sampling Method with Separated Deposition of Airborne Fibers and Other Particles. J. Aerosol Sci., 8:205, 1977.

17. Timbrell, V. J. Appl. Phys. 43:4839, 1972.

18. Binek, B., and B. Dohnalova. A New Aerosol Particle Analyzer. Collection Czechosnov, Chem. Comm., 36:954, 1971.

19. Binek, P. Properties and Applications of the Scintillation Particle Counter. Staub., 30:31 (Engl. trans.), 1970.

20. Freedman, R. W., S. Z. Toma, and W. H. Lang. On-Filter Analysis of Quartz in Respirable Coal Dust by Infrared Absorption and X-Ray Diffraction. AIHA Journal, 35:411, 1974.

21. Wagman, J., R. L. Bennett, and T. Knapp. X-Ray Fluorescence Spectrometer for Rapid Elemental Analysis of Particulate Pollutants, Emissions Measurement and Characterization Division. EPA Environmental Sciences Research Laboratory, EPA-600/2-76-033, 1976.

22. Wagman, J., R. L. Bennett, and K. T. Knapp. Simultaneous Multiwavelength Spectrometer for Rapid Elemental Analysis of Particulate Pollutants. In: X-Ray Fluorescence Analysis of Environmental Samples, T. G. Dzubay (ed.), Ann Arbor Science Publishers, Inc., Ann Arbor, Michigan, 1977.

23. Van de Hulst, H. C. Light Scattering by Small Particles. J. Wiley and Sons, Inc., p. 304. 1957.

24. Spurny, K., C. Boose, and D. Hochrainer. Zur Zerstaubung von Asbestfasern in einem Fliessbett-Aerosol Generator. Stab., 35:440, 1975.

25. Rosen, H., et al. Identification of the Optically-Absorbing Component in Urban Aerosols. App. Opt., 17:3859, 1978.

26. Yasa, Z., et al. Photoacoustic Investigation of Urban Aerosol Particles. App. Opt., 18:2528, 1979.

27. Chan, C. H. Effective Absorption for Thermal Blooming due to Aerosols. App. Phys. Lett., 26:628, 1795.

28. Terhune, R. W., and J. E. Anderson. Spectrophone Measurements of the Absorption of Visible Light by Aerosols in the Atmosphere. Opt. Let., 1:70, 1977.

29. CRC Press. Handbook of Chemistry and Physics. 59th Ed. 1978.

30. Knollenberg, R. G., and R. Luehr. Open Cavity Laser "Active" Scattering Particle Spectrometry. In: Proceeding Symposium on Fine Particles, EPA-600/2-75-059, p. 669, October 1975.

31. Schuster, B. G., and R. Knollenberg. Detection and Sizing of Small Particles in an Open Cavity Gas Laser. App. Opt., 11:1515. 1972.

BEGIN FIRST LINE OF TEXT HERE
TYPING GUIDE SHEET
CENTER OF PAGE
TOP OF IMAGE AREA
DROPPED HEAD; BEGIN SECTIONS HERE

BIBLIOGRAPHY

An important effort within this program was to perform an exhaustive literature search on the general subjects of carbon and graphite fiber release into the atmosphere, as well as applicable monitoring techniques. The search for emission information resulted in very limited data principally because of the incipient nature of this industry and the paucity of any systematic work on source characterization. The main body of information on carbon fiber emissions (or the lack of such emissions) from industrial operations involving such materials came from spokesmen within these industries rather than from data in the open literature. Thus, the validity of such information must be viewed in the context of its source whose verification is, at best, difficult. In view of this situation, it appears desirable to subject a representative sample of such industrial operations to an impartial and objective monitoring program whose objective would be to either confirm the assessment provided by such industries or, alternatively, to establish that carbon fiber emissions are of environmental significance.

The search for applicable detection and monitoring techniques required a two-prong attack. On one hand, those methods developed specifically for carbon fiber monitoring had to be identified, and on the other, potentially applicable or candidate techniques had to be selected, whose development into carbon fiber-specific instrumentation warranted their consideration.

The literature search used the computer services of the New England Research Applications Center (NERAC) at the University of Connecticut. The initial search was performed by using the following list of key words:

Carbon Fiber	Aerosol
Carbon-Fiber	Wind
Carbon Fibre	Wind-
Carbon-Fibre	Wind/
Graphite Fiber	Airborne
Graphite-Fiber	Pollution
Carbon	Sensing
Graphite	Sensor
Fiber	Detect
Fibre	Monitor
Air	Identif
Air-	

BEGIN LAST LINE OF TEXT
3/8"
BOTTOM OF IMAGE AREA OUTSIDE DIMENSION FOR TABLES AND ILLUSTRATIONS

PAGE NUMBER
EPA-287 (Cin.)
(4-76)

BEGIN FIRST LINE OF TEXT HERE
TYPING GUIDE SHEET
CENTER OF PAGE
TOP OF IMAGE AREA
DROPPED HEAD; BEGIN SECTIONS HERE

Later on, as the photothermal carbon fiber detection and characterization scheme was being evolved, an additional list was compiled in order to uncover any relevant information of that method and related investigations. This additional list of key words was as follows:

Photothermal Spectrosc	Aerosol
Photothermal Spectrosc	Detect
Photo-Thermal Spectrosc	Sensor
Photoacoustic Detect	Partic
Photo-Acoustic Detect	Air Pollut
Optoacoustic Detect	Pollut
Photothermal	Fiber
Photo-Thermal	Fibre
Spectrosc	Airborne
Photoacoustic	Density
Photc-Acoustic	Anal
Optoacoustic	Emission
Opto-Acoustic	Spectr

In addition to the computerized NERAC search, the personnel assigned to this program pursued their own lines of literature investigations, with the active support of the GCA/Technology Division librarian group. Awareness of related and relevant literature, not always uncovered by the computerized search, provided a very necessary complement to that search.

Several of the most important publications are referenced directly in the preceding sections of this report and will not be repeated here. Additional relevant bibliography, however, is included in this section. Some of these references are presented with an abstract or short summary, whenever the information warrants such a distillation.

BEGIN LAST LINE OF TEXT
BOTTOM OF IMAGE AREA OUTSIDE DIMENSION FOR TABLES AND ILLUSTRATIONS
3/8"

PAGE NUMBER
EPA-257 (Cin.)
(4-76)

1. Adamowicz, R. R., and K. P. Koo. 1979. Characteristics of a Photoacoustic Air Pollution Detector at CO_2 Laser Frequencies. NAS 21-35, Applied Optics. 18:2938-2946.

The characteristics of a photoacoustic detection system for measurement of ambient trace atmospheric pollutants are described as well as an alternative traverse acoustic cell to eliminate cell window signals. The techniques for minimizing effects of trace gas interferents are reported.

2. Anderson, J. E., and T. J. Truex. Mass Monitoring of Carbonaceous Aerosols with a Spectrophone. U.S. DOE Contract No. W-7405-ENG-48.

The feasibility of using light absorption as in in-situ mass monitor for carbonaceous aerosols has been studied. Findings: (1) spectrophone output is proportional to carbonaceous aerosol mass concentration, (2) absorption coefficient of carbonaceous aerosols is 17 m^2/gm at 4166 Å. The spectrophone as a means to monitor carbonaceous aerosols is far less time-consuming than filter collection techniques.

3. Anderson, J. E., and R. W. Terhune. 1977. Spectrophone Measurements of the Absorption of Visible Light by Aerosols in the Atmosphere. Optics Letters. Vol. 1.

An acoustically resonant spectrophone was used to measure the absorption and scattering by aerosols in ambient room air with the addition of large amounts of aerosols.

4. Anderson, J. E., and R. W. Terhune. 1977. Spectrophone Measurements of the Absorption of Visible Light by Aerosols in the Atmosphere. Opt. Lett. (USA). 1(2):70-2.

The basis of spectrophone measurement system: Detection of sound waves generated by localized time dependent heating of the air is described. The spectrophone and means of isolating it from room noise is shown diagramatically. Aerosol extinction coefficients are tabulated for NACL, NICL/Sub 2/and cigarrette smoke aerosols.

5. Bard, A. J. 1978. Photoacoustic and Photothermic Spectroscopy. Publication Class Journal. No. 208426, Analysis. 6:277-83.

6. Baykoov, B. K., M. Y. Berlyand, R. W. Gildenskiold, R. I. Onikul, G. A. Panfilova, and I. M. Zrazherskiy. Scientific Translation Service, Santa Barbara, California.

The research to expand the applicability of the standard method for calculating the dispersion of industrial emission in the atmosphere is reported.

7. Beheshti, M. 1966. The Adsorption and Scattering of Radiation by Solid Carbon Particles. AIAA Paper No. 66-134, Third Aerospace Sciences Meeting, NY.

8. Benin, D., S. H. Lin, T.A. Moore, and R. Tom. 1979. A Thermal Diffusion Model of Photothermal Spectroscopy. Chemical Physics Letter. 66(2).

A phenomenological theory of Photothermal Spectroscopy (PTS) is developed in which the temporal behavior of the PTS Signal can be described and the relationship between the ordinary absorption spectra and PTS spectra is determined.

9. Berger, H. R., W. D. Conner, J. L. Miller, and J. Wagman. 1979. Dusts and Residues from Machining and Incinerating Graphite/Epoxy Composites. EPA-600/2-79-196.

Examination of graphite/epoxy residues from machining and incineration showed the graphite fibers had high resistance to combustion up to 1000°C. Using conventional refuse incineration would result in the release in large amounts of graphite fibers. There is also potential for fibers that are respirable when sawing graphite.

10. Bernal, J. D. 1924. The Structure of Graphite. Royal Society of London, Proceedings. 106.

11. Bernstein, J. B., D. Kirk, K. L. Stierwalt. 1963. Applied Optics. 2.

This discusses a comparison between a spectrophotometer and a black-body method at the same temperature. The results indicated that the spectrophotometer IR technique is particularly good for measuring low absorption coefficients.

12. Boni, A. A. 1974. Actual Investigation of Laser Supported Combustion Waves. Part 2: Measurements of the Effect of Particulate Matter on Air Breakdown by 1.06 micron. Report No. AD-784-356, Army Missile Command.

Studies were conducted to determine the effect of particulate matter (SiO_2 and carbon fibers of various diameters) on laser-induced air breakdown.

13. Bowse, B. M., G. L. Hagnaver, and J. M. Murray. HPLC Monitoring of Graphite Epoxy Prepregs. Report No. AD-A072294-Avail. NTIS.

A method using high performance liquid chromatography has been developed for the quality control of graphite-epoxy prepregs. The method is used to monitor compositional changes as the prepreg ages. Chemical changes in the prepreg are correlated with aging time and process acceptability.

14. Brannan, W. I., J. A. Morrissey, S. C. Thompson. 1978. Calibration of BRL Ball and Sticky Cylinder Detector Systems. ARBL-TR-02079.

The procedure for calibration of the BRL (brass ball) detection system for a thin conductor length, concentration, and exposure is discussed. The calibration of the sticky cylinder detectors for 7 mm length is also discussed.

15. Bucher, W. 1977. Electrostatic Forces on Conductors Moving Between Conducting Plates. Report No. BRL-1977, USA. Ballistic Research Ctr. Lab, Aberdeen Proving Ground, Maryland.

16. Bucher, W. 1976. On the Phenomenon of Current Pulses Generated by Conductors Near Contact in Electrical Fields. Rep. No. BRL-1951, USA Ballistic Research Lab., Aberdeen Proving Ground, Maryland.

This paper describes a method to detect conducting particles and conductor leakage by generation of current pulses in external circuitry by neutral or charged conductors.

17. Burton, G. S., and R. Knollenberg. 1972. Detection and Sizing of Small Particles in an Open Cavity Gas Laser. Applied Optics. 11.

Using two traverse modes of a (He-Ne gas laser) TEM_{00} and TEM^{01} a plot of particle extinction loss vs. laser power was made. It was in accordance with the theory for an inhomogeneously broadened line under the condition of small saturated gain per pass.

18. Chan, C. H. 1975. Effective Absorption for Thermal Blooming Due to Aerosols. Applied Physics Letters. 26.

Thermal blooming on laser propagation due to the presence of aerosol particles is discussed. It is found there is a small time delay in thermal blooming due to the time delay for the air to heat.

19. Colles, M. J., and N. R. Geddes. 1979. The Optoacoustic Effect. Contemporary Physics. 11-36.

The generation of acoustic signals following optical absorption in gases and solids is described. Examples are given of important applications of the optoacoustic effect in pollution monitoring, the measurment of lifetimes and gas-phase and solid state spectroscopy.

20. Copen, L., R. Gray, and H. Wolf. 1979. Carbon Fiber Electrical Effects Evaluation Methodology. Naval Surface Weapons Center.

Research in the areas to define the properties and interactions of typical carbon/graphite fibers to evaluate the seriousness of adverse effects on electrical and electronic equipment.

21. Eckstein, B. The Rate of Oxidation of Carbon Fibers in Air. Union Carbide Corp., Center, Carbon Products Div., Parma Technical Center, Parma, OH.

Carbon fibers made from PAN, rayon were kept in circulating air ovens for 1000 hours at temperatures between 230 and 315°C. The PAN-based yarns oxidized more rapidly.

22. Egan, D. M., and J. H. Williams, Jr. 1978. Acoustic Emission Spectral Analysis of Fiber Composite Failure Mechanisms. Report No. NSG-2938, Lewis Res. Center.

A study of acoustic emission characteristics of graphite fiber polymeric composites by SCM analysis determined predominant individual failure mechanism.

23. Freeman, J. J., R. M. Friedman, and H. SL Reichard. 1980. Photoacoustic Spectroscopy of Particulate Solids. J. Phys. Chem. 84: 315-319.

Photoacoustic and diffuse reluctance spectra of powdered solids in defined particle size distributions were investigated. The study showed a close parallel between the photoacoustic (PA) and diffuse relectance (DR) measurements on the solids. Their recommendation was that an analysis similar to Kubelka-Munk treatment of DR data be applied to PA measurements on particulate solids.

24. Faxvog, F. R., and D.M. Roessler. 1979. Optoacoustic Measurement of Optical Absorption in Acetylene Smoke. J. Opt. Soc. Am. 69.

It was found that specific absorption coefficients were 8.3 ± 0.9 and 0.76 ± 0.1 m^2 g^{-1}, for acetylene smoke in a nonresonant cell at wavelengths 0.5145 and 10.6 μm. This experimentally determined the responsibility of the optoacoustic cell which was used to take the measurements.

25. Grogen, D. L. 1980. Toxic Hazards of Air Force Nonmetallic Materials. Aerospace Medical Research Lab, Wright-Patterson AFB, Ohio, DTIC Rpt. No. BLLBOK-6302.

Physical and chemical behavior of nonmetal materials is being investigated under various conditions to ascertain their potential toxicity in confined spaces. No results are given.

26. Gundel, J., A. D. A. Hansen, T. Novakov, and H. Rosen. 1978. Identification of the Opacity Absorbing Component in Urban Aerosols. Applied Optics. 17.

Using Raman Spectroscopy to identify and characterize air pollution particulates. It has successfully been able to determine the graphite species in the air. It was found that the absorbing species in urban source particulate samples is graphitic soot.

27. Heimbuch, A. 1979. Fire Resistant Materials. National Aeronautics and Space Admin., Ames Research Center, Moffett Field, Calif., DTIC Rpt. No. BLL30K-505.

Research is being conducted to provide improved source properties and fire safety for both domestic and military application of carbon-graphite fiber material. These include resin matrix binders, film, formens, form adhesives, etc.

28. Hawthorne, H. M. 1971. Structure and Properties of Strain-Graphitized Glassy Carbon Fibers. Center for Materials Research, Univ. of British Columbia, Vancouver, Canada, Paper No. 12, International Carbon Fibers Conference, London, England.

29. Huang, Y. Instrument Society of AMSEC class. The ADEH Model of Carbon Fibers as an Air Pollutant. Tenth Annual Pittsburgh conference on modeling and simulation, conference paper, U.S. Army Ballistic Research Lab.

Carbon/graphite fiber reinforced thermoplastics are the fastest growing class of composite materials for the aerospace and sporting goods industries. However, millions of fibers can be released from the materials when burnt or exploded. The airborne fibers pose a potential problem of air pollution and can cause electrical malfunctions. The current state of the art and attempts to enhance the understanding of the ADEM of carbon fibers from an analytical approach.

30. Intergovernmental Committee, National Aeronautics and Space Admin. 1978. Carbon Fiber Study.

As usage of carbon/graphite fiber materials increases (worldwide production 1978-700,000 pounds, 1990 est. 1 billion) the possibility of accidental release during manuacture or by destruction is a major hazard, (i.e., shorting or arcing of electrical equipment). As for having an impact of human health, their impact is not yet known. Further investigations are recommended.

31. Japar, S. M., and D. K. Killinger. 1979. Photoacoustic and Absorption Spectrum of Airborne Carbon Particulate using a tunable Dye Laser. Chem. Phys. Letter. 207-9. CA Vol. 092, No. 063818.

32. Johnson, R. L., J. D. Lindberg, S. A. Schleusener and K. O. White. 1976. Spectrophone Measurements of Infrared Laser Energy Absorption by Atmospheric Dust. Applied Optics. 15.

A new method to quantitatively measure the absorption of atmospheric dust is described. The ranges used are from UV to far IR in wavelength using a differential spectrophone KB and Pellet technique.

33. Kakeklar, A. S. 1979. An Assessment of the Dusts Resulted by the Use of Carbon Fiber Composites in Commercial Aviation. Vol. 1: Final Report, Vol. 2, Supporting Appendices, NASA Contract NAS1-15380.

34. Kanstad, S. O., and P. E. Nordal. 1979. Photoacoustic and Photothermal Spectroscopy - Novel Tools for the Analysis of Particulate Matter. No. 154101, Powder Technology 1979. pp. 133-7.

Measurements on powders using Photoacoustic (PAS) and Photothermal (PTS) spectroscopic techniques are described. Three different techniques are used to analyze and identify the sample through its absorption spectrum. The advantages of using PAS and PTS methods to powder analysis are presented and their applications to in-stream measurements of particulate solid properties are discussed.

35. Kaye, B. H., A. G. Naylor, N. I. Robb, and V. Timbrell. 1976. Reprocessing of Fibers for Efficient Characterization by Pattern Recognition Technology. Powder Tech. 14: 189-190.

Carbon, asbestos, and other man-made fibers undergo alignment in magnetic fields. This alignment reduces the overlapping of linear fibers. They can be given a distribution for length and diameter by using the Omnicon Pattern Analysis System.

36. Krishnan, K. S. 1974. Magnetic Anistropy of Graphite. Nature (Land). 133: 174-175.

37. Laude, L. S., and J. D. Lindberg. 1974. Measurement of the Absorption Coefficient of Atmospheric Dust. Applied Optics. 13.

Their work used an already-developed method for powder materials to measure the absorption of atmospheric dust. The Kubelka-Munk theory of diffuse relectance was used on the dust which corresponded with those of other results conducted by different methods.

38. Matthauser, E. E. 1979. Advanced Aircraft Structure. National Aeronautics and Space Administration, Langley Res. Ctr., Langley, Virginia, DTIC Report No. BLL30K-505-33.

Part of this study is to determine environmental effects of degradation of graphite/carbon fiber composites.

39. McLelland, J. F., and R. N. Kniseley. 1978. Photothermal Conversion Surface Measurements Using Photoacoustic and Photothermal Spectroscopics. Dept. of Energy-JRNL.

Measurements are made by modulating the intensity of an incident light beam which causes a temperature oscillation in the irradiated material, where the oscillation amplitude is proportional to the absorbed and subsequently thermalized light energy. In the photoacoustic method, the oscillation amplitude is measured by a transducer which detects an acoustical signal driven by the temperature oscillation.

40. Meyers, J. A. The Transfer of Carbon Fibers Through a Commercial Aircraft Water Separator and Air Cleaner. Journal, Vol. and Issue S1805, NASA-CR-159183.

The fraction of carbon fibers passing through a water separator and an air filter was determined in order to estimate the proportion of fibers outside a closed aircraft that are transmitted to the electronics through the air conditioning system.

41. Morrissey, J. A., and R. D. Shelton. Electronic Detector for Conducting Particles and Fibrils.

Small airborne conducting particles and fibrils strike a conducting surface with an electric charge distribution on it, they acquire charge and are repelled from the surface. A brass ball detector is used to collect the charging pulses which can then be processed by a pulse height analyzer to yield information on the airborne particles.

42. National Aeronautics and Space Administration. A Report of Observed Effects on Electrical Systems of Airborne Carbon/Graphite Fibers. Washington, DC, NASA Report No. TM-78652.

Release of free carbon/graphite fibers can cause potential hazards to electrical systems, and manufacturers and workers should exercise caution in their use and disposal.

43. National Aeronautics and Space Admin. 1978. A Report of Observed Effects on Electrical Systems of Airborne Carbon Graphite Fibers. NASA-Washington, DC, NASA Dept. No. TM-78652.

44. Novakov, T., (Editor). 1978. Carbonaceous Particles in the Atmosphere. Proceedings - Dept. of Energy, No. W-7405-ENG-48.

Compilation of papers presented at the meeting held at Lawrence Berkeley Lab, Univ. of Calif.

45. Parry, J. L., and J. S. Dierose. 1979. RADC Carbon Fiber Test Facility. RADC-TR-79-107. Romie Air Development Center, AFSC, Griffis Air Force Base, NY.

Vulnerability of electronic equipment to air transportable carbon fibers was evaluated.

46. Photoacoustic spectroscopy symposium, Ames, Iowa, Aug. 1979. Technical Digest Monchalin, Jean-Pierre, Gagne, Jean-Marie, Luc Parpal, Jean, Bertrand, Lionel.

Digest of technical papers presented at the Topical Meeting on Photo-acoustic Spectroscopy.

47. Rosen, H., A. D. A. Hansen, R. L. Dod, and T. Novakov, 1978. Application of the Optical Absorption Technique to the Characterization of the Carbonaceous Component of Ambient and Source Particulate Samples. American Chemical Society, pp. 640-643.

The carbon content and optical absorption of the particulates were found to show a strong correlation. The results suggest that the absorptivity is due to "graphitic" soot and that major fraction of the ambient carbonaceous aerosols in the investigated episodes is primary in origin.

48. Sharp, J. V., and S. G. Burnay. 1971. High Voltage Electron Microscopy of Internal Defects in Carbon Fibers. Metallurgy Division, Atomic Energy Res. Estab., Harwell Paper No. 10, International Carbon Fibers Conference, London, England.

Use of high-voltage electron microscopy to measure internal flows of fibers while in transmission with sizes greater than 0.1 micrometers.

49. Soderqvist, R., E. Elvers, and M. Larson. Method of Determining Small Shift in X-Ray Reflections Detected by Parallel Scanning. Res. Inst. of National Defense, Sweden.

The reflection for a reference material is recorded by a position-sensitive sensor. The changes in the appearance of the reflection are then calculated from different curves. The method is illustrated by experiments using test rods of aluminum and carbon-fiber reinforced laminated plastic.

50. Sussholz, B. 1978. Evaluation of Micron Size Carbon Fibers. TRW Division and Space Systems Group, NASA-1-45465.

Tests were conducted to determine quantitative estimates as to the presence of micron-sized carbon fibers released during the burning of graphite composites. Increased fiber oxidation occurred after a propane burn closely followed by the introduction of a wind source.

Measurements were taken with a scanning electronic microscope. Results revealed that a burn would result in concentration levels of about half of the OSHA asbestos limit.

51. Talbot, J. H. 1966. A Diffraction Size-Frequency Analyzer with Automatic Recording of Size-Frequency Distributions and Total Respirable Surface Areas. Journal of Scientific Instrumentation.

52. Timbrell, V. 1972. Alignment of Carbon and other Man-Made Fibers by Magnetic Fields. Medical Research Council, Pneumoconiosis Unit, Landough Hospital, Penarth, S. Wales, United Kingdom.

Graphite, a High Modulus Carbon Fiber in liquid suspension, shows a parallel alignment by a magnetic field. It is shown that these fibers sediment at a slow rate allowing ample time for observation.

53. Timbrell, V. 1965. The Inhalation of Fibrous Dusts. Academy of Science. 132.

Although the largest particles usually found in lungs are 10 micrometers in diameter, asbestos fibers of 50 and 200 micrometers long are found. This is found because a main mechanism of deposition is particle free falling speed which is mostly determined by the particle diameter. A fiber of asbestos with a diameter less than 3.5 microns has a good chance of penetrating deep into the lungs and deposit in places where respiratory bronchioles branch.

54. Wagman, J. 1979. Dusts and Residues from Machining and Incinerating Graphite/Epoxy Composites. Emissions Measurement and Characterization Division, ESRL, Research Triangle Park, North Carolina, Report No. EPA 600/2-79-196.

Experiments conducted in the laboratory shows that incineration by conventional methods would result in both intact and partially thinned and/or degraded fibers and that resistance to combustion exists up to 1000°F. Machining operations on graphite fibers (i.e., cutting and griding) can cause generation of fibers with a dimension of less than 10 micrometers whereas sawing and drilling operations usually result in fibers less than 100 micrometers. These studies were done utilizing scanning electron microscopy.

55. Watt, W. 1970. Production and Properties of High Modulus Carbon Fibers. Proceedings Royal Society of London - A.319.

56. Wentworth, S. E. 1974. Army Materials and Mechanics Research Center, Watertown, MA, AMMRETR79-1.

57. Yang, L. C. 1980 High Voltage Spark Carbon Fiber Detection System. JPL Publication 80-30, NASA.

This discusses the development of a high voltage spark detection system to determine the density and length of carbon fibers in the air from a fire or crash of aircraft. It is based on the ability of a carbon fiber to initiate spark discharges across a high voltage biased grid. The design was proved satisfactory and some prototypes were used in field and laboratory tests.

58. Yasa, Z., N. M. Amer, H. Rosen, A. D. A. Hansen, and T. Novakov. 1979. Photoacoustic Investigation of Urban Aerosol Particles. Applied Optics. 18.

The photoacoustic analyzer results in sampling of aerosol particles were compared with results of the Raman spectroscopy sampling of aerosols done previously. The conclusion was that the optically absorbing component of urban aerosol particles is graphitic carbon.

59. Yasa, Z., N. M. Amer, H. Rosen, A. D. A. Hansen, and T. Novakov. 1979. Photoacoustic Investigation of Urban Aerosol Particles. Applied Optics (USA). 18(15): 2528-30

Results presented, combined with Raman Scattering data and thermal analysis and solvent extraction results, indicate that the optically absorbing component of urban aersol particles is graphitic carbon.

60. Office of Naval Res. Carbon Fiber Study Group. 1978. Fiber Electrical Resistance Modification - Its Relationship to Electrical Equipment Malfunction. The Aerospace Corp., Elsequado, CA, Report No. TR-0079(3721-11)-1. Recommendations from this study include:

- Risk analysis should be expanded to include all current and potential major application in both military and general use.
- Information on all aspects of carbon fibers manufactured, usage, and disposal should be centrally organized and communicated to users of the product.
- Methods should be investigated to dispose of carbon fibers that are safe both now and in the future.